Review

Indole-Based Metal Complexes and Their Medicinal Applications

Zahra Kazemi *, Hadi Amiri Rudbari *, Nakisa Moini, Fariborz Momenbeik, Federica Carnamucio, Nicola Micale *

Posted Date: 20 December 2023

doi: 10.20944/preprints202312.1571.v1

Keywords: Indole; metal complexes; medicinal applications; biological activity

Review

Indole-Based Metal Complexes and Their Medicinal Applications

Zahra Kazemi [1,*], Hadi Amiri Rudbari [1,*], Nakisa Moini [2], Fariborz Momenbeik [1], Federica Carnamucio [3] and Nicola Micale [3,*]

[1] Department of Chemistry, University of Isfahan, Isfahan, 81746-73441, Iran; zahrakazemy85@yahoo.com (Z.K.); hamiri1358@gmail.com (H.A.R.); f.momen@chem.ui.ac.ir (F.M.).
[2] Department of Chemistry, Faculty of Physics and Chemistry Alzahra University, P.O. Box 1993891176, Vanak Tehran, Iran; n.moini@alzahra.ac.ir (N.M.).
[3] Department of Chemical, Biological, Pharmaceutical and Environmental Sciences, University of Messina, Viale Ferdinando Stagno D'Alcontres 31, I-98166 Messina, Italy; carnamuciof@unime.it (F.C.); nmicale@unime.it (N.M.).
* Correspondence: zahrakazemy85@yahoo.com (Z.K.); hamiri1358@gmail.com (H.A.R.); nmicale@unime.it (N.M.).

Abstract: The indole nucleus is an important element of many natural and synthetic molecules with significant biological activity. Nonetheless, the co-presence of transitional metals in organic scaffold may represent an important factor in the development of effective medicinal agents. This review covers some of the relevant and recent achievements in the biological, chemical and pharmacological activity of important indole-based metal complexes in the area of drug discovery.

Keywords: Indole; metal complexes; medicinal applications; biological activity;

1. Introduction

Structurally, indole is a planar bicyclic molecule in which a benzene ring is fused to the 2,3-positions of a pyrrole ring (Figure 1). According to Huckel's rule, indole is aromatic in nature [1]. In 1866, indole was synthesized for the first time by Adolf von Baeyer from the oxidation of indigo [2]. Since then, a variety of synthetic strategies have been developed for the preparation of the indole nucleus [3-6], including the Bischler-Möhlau [7], Fischer [8], Hemetsberger [9], and Julia synthesis [10]. In addition, various indole derivatives can be synthesized by substituting the indole ring at the N-1, C-2 to C-6, or C-7 positions with the ultimate goal of improving its characteristics [11].

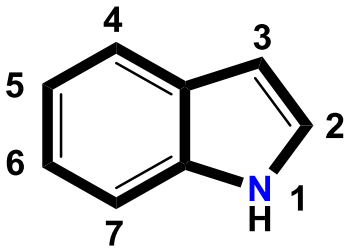

Figure 1. Illustration of the structure of the indole nucleus with relative numbering.

The indole scaffold is known to be a key structural component of some classes of FDA-approved drugs such as the vinca alkaloids vinblastine and vincristine and the related semi-synthetic derivatives vindesine and vinorelbine (for the treatment of various types of cancer), physostigmine (for the treatment of Alzheimer's disease and glaucoma), and alkaloids of the *Rauvolfia* species including ajmaline (1-A anti-arrhythmic agent), ajmalicine and reserpine (antihypertensive drugs) [12-14]. Furthermore, the presence of the pyrrole ring in the structure of indole makes the latter an electron-rich aromatic scaffold with distinctive binding properties, many of which occur with target-receptors belonging to the class of integral membrane G-protein coupled receptors (GPCRs) via

Preprints (www.preprints.org) | NOT PEER-REVIEWED | Posted: 20 December 2023 doi:10.20944/preprints202312.1571.v1

complementary interactions with conserved binding pockets [15, 16]. Like other heterocycles, indole is regarded as a main constituent of biomolecules and natural products endowed with outstanding properties. Tryptophan (Trp), an essential amino acid, is one example of them whose structure possesses an indole nucleus near the active site of metalloenzymes involved in electron-transfer pathways [17, 18]. Other important examples include the phytohormone of the auxin class indole-3-acetic acid (IAA) and the metabolites/nutrients indole-3-carbinol (I3C) and 3,3'-diindolylmethane (DIM) which derive from the breakdown of the glucosinolate glucobrassicin present in high levels in vegetables of the *Brassicaceae* family (Figure 2).

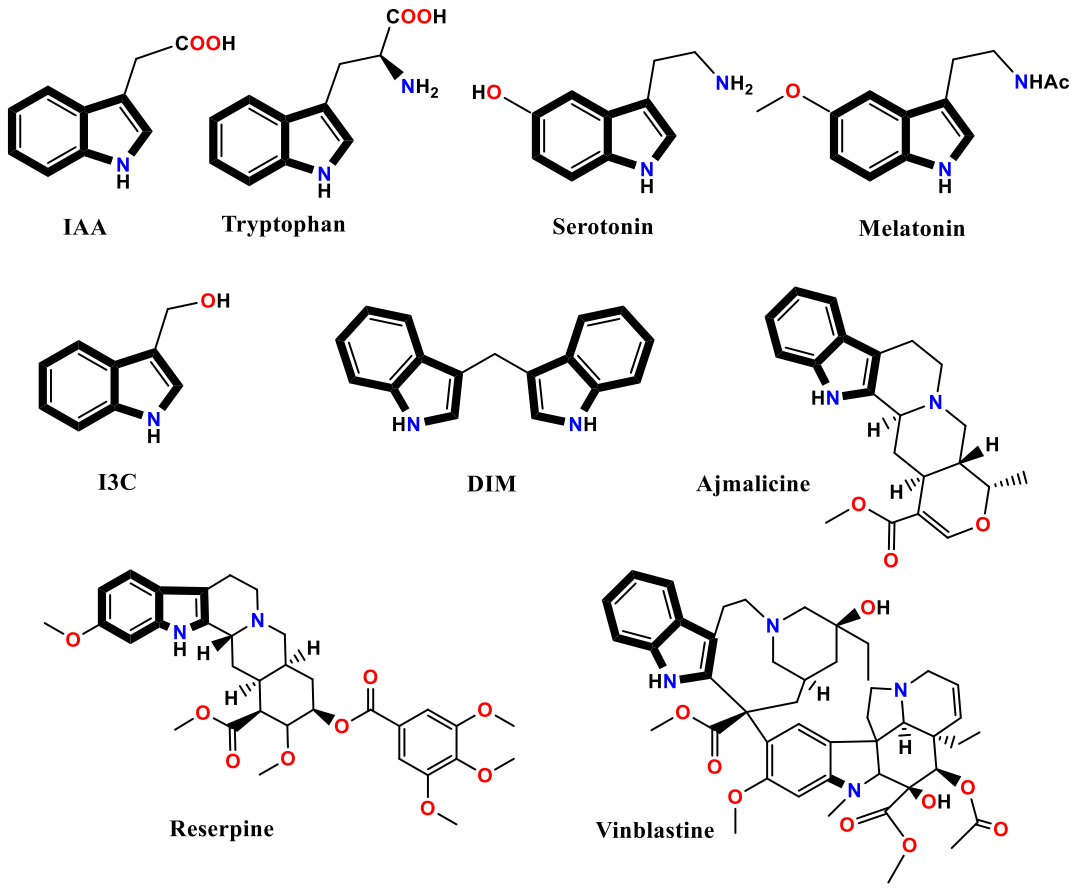

Figure 2. Examples of indole-containing natural products and drugs.

Additionally, indole is regarded as a privileged molecular scaffold due to its presence in a wide range of pharmacologically active molecules and its ability to interact efficiently with multiple receptors besides GPCRs [19]. This wide range of biological activities of the indole scaffold includes antibacterial [20], anti-tubercular [21], α-amylase and monooxime inhibition [22], antiprotozoal [23], and anti-tumor activity [24]. Therefore, attempts to exploit this unique scaffold have attracted great attention from scientists. For instance, A. M. Bianucci *et al*. reported the key role of the indole N-H group in the interaction with specific receptors. Indeed, the isosteric replacement of the indole scaffold with a benzothiophene or benzofuran in a series of glyoxylylamine derivatives resulted in a decrease of the affinity for benzodiazepine receptors (Figure 3) [25].

Preprints (www.preprints.org) | NOT PEER-REVIEWED | Posted: 20 December 2023 doi:10.20944/preprints202312.1571.v1

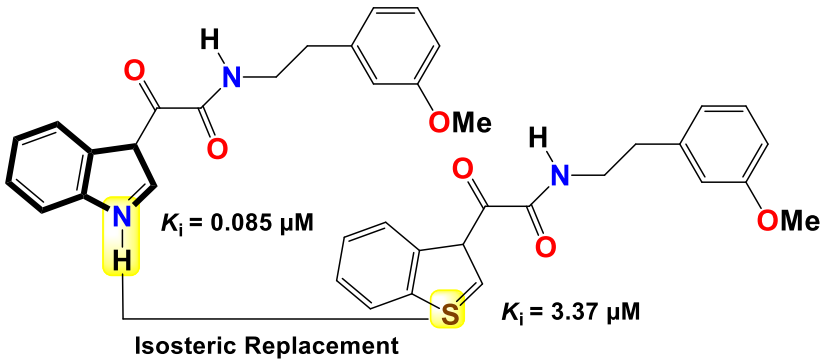

Figure 3. Example of effective isosteric replacement involving the indole scaffold towards binding affinity for benzodiazepine receptors. .

The indole scaffold has also been successfully employed for the preparation of macrocyclic structures which turned out to be effective as antimicrobial and anticancer agents [26-32]. Indole has been extensively studied in the context of the catalytic asymmetric synthesis for the development of indole-based chiral heterocycles, another important class of compounds that can be found in numerous pharmaceuticals, natural products, functional materials, chiral catalysts and ligands [33]. Nevertheless, indole derivatives have gained importance in the design and development of drugs to treat a variety of neurodegenerative disorders since the discovery of the indole derivative NC008-1 [34-37].

The pharmacological properties of these heterocyclic compounds can be considerably improved by increasing their solubility and bioavailability which can be accomplished through the formation of complexes with a variety of transition metal cations [38, 39]. Indeed, the coordination behavior of indole derivatives with transition metal ions has recently attracted the attention of researchers, and myriad publications using these compounds as ligands have been reported [40-43]. Koji Yamamoto et al. [44] reported different patterns of coordination of the indole rings with metal centers. They hold an opinion that pure σ-complexes are not always formed in indole–metal complexes; there is also the possibility of σ/π-intermediates (B) and π-modes (C or D) (Scheme 1). As a matter of fact, indole can exists in two tautomeric forms, 1*H*- and 3*H*-indole (Figure 4) [45]. 3*H*- and 1*H*-indole behave differently toward metal ions since (N(1)) in the former, which is considered as an imine nitrogen, has the coordinating ability, while the pyrrole moiety of 1*H*-indole is capable of forming salts with alkali metal ions by deprotonation. The different types of bonding of the indole ring with transition metal ions have been reported. For instance, a σ-bond between Pd(II) and the pyridine-like nitrogen of the 3*H*-indole tautomer was stated for the first time [46]. Apart from this, a number of noncovalent interactions of indole rings with other molecules has been observed via hydrogen bonding, π–π stacking and cation–π interactions [45].

Preprints (www.preprints.org) | NOT PEER-REVIEWED | Posted: 20 December 2023 doi:10.20944/preprints202312.1571.v1

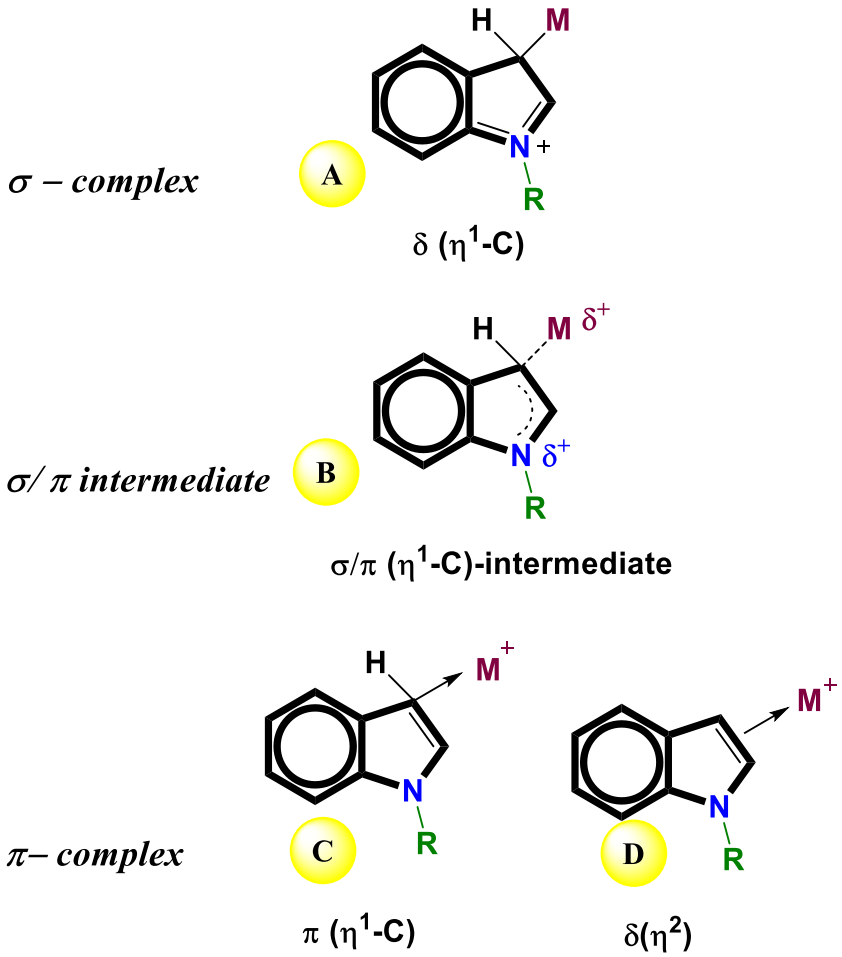

Scheme 1. Different patterns of coordination of the indole rings with metal centers.

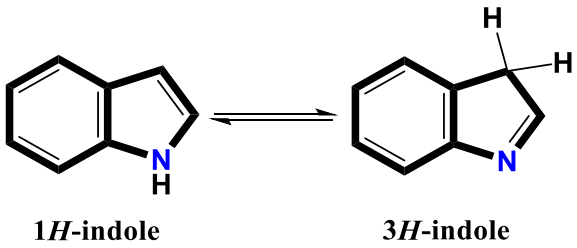

Figure 4. Tautomeric forms of indole.

Starting from these premises, we focused this review article on synthesis, description of structural features and biological activity of indole-based metal complexes.

2. Monodentate ligands

2.1. N-donor

Novel ligands, namely N-alkylindole-substituted 2-(pyrid-3-yl)-acrylonitriles (**L1a-L1e**; Scheme 2), were recently used for the preparation of (p-cymene)Ru(II) piano-stool complexes (i.e. **1a-1e**; Scheme 2) [47]. The synthesis of these compounds was achieved through the replacement of the isovanillyl and veratryl moieties of known anticancer tyrphostin derivatives with the indole scaffold, with the aim of enhancing their biological activity profile. The in vitro cytotoxicity of the ligands and related complexes against HCT-116 colorectal carcinoma (both p53-wildtype and p53-knockout cells) and MCF-7 breast cancer cell lines was investigated by MTT assay. Among the ligands, **L1a** and **L1b** turned out to be the most potent derivatives against MCF-7 cells (IC_{50} in the low-micromolar range)

Preprints (www.preprints.org) | NOT PEER-REVIEWED | Posted: 20 December 2023 doi:10.20944/preprints202312.1571.v1

and the two HCT-116 cell lines (IC_{50} in the sub-micromolar range), respectively. The anticancer activity of the complex **1a** was higher than its ligand and the reference drugs sorafenib, gefitinib, and NAMI-A. Additionally, the authors studied the interaction between the most active compounds **L1a**, **L1b** and **1a** with DNA using the ethidium bromide intercalation assay, demonstrating high binding affinity for the complex **1a** and no DNA binding for the ligands **L1a** and **L1b**. Additionally, a number of other experiments have been carried out, including the investigation of drug mechanisms in HCT-116 p53-knockout colon cancer cells, colony formation assays, experiments with tumor spheroids and molecular docking. Overall, these studies underlined that indole scaffold was essential for the high antiproliferative activity [47].

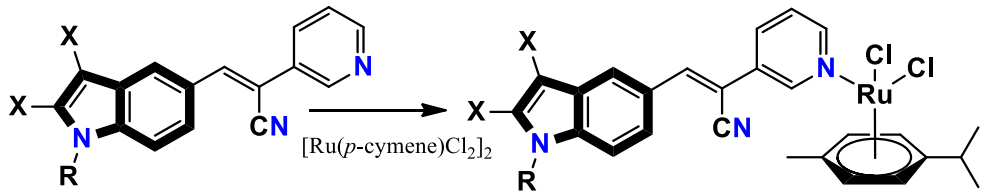

L1a: R = Me, X = H
L1b: R = Et, X = H
L1c: R = Et, X = Cl
L1d: R = Pr, X = H
L1e: R = CH_2CCH, X = H

1a: R = Me, X = H
1b: R = Et, X = H
1c: R = Et, X = Cl
1d: R = Pr, X = H
1e: R = CH_2CCH, X = H

Scheme 2. Synthesis of (p-cymene)Ru(II) piano-stool complexes **1a-1e**.

2.2. S-donor

In 2018, Ashiq Khan et al. [48] prepared and characterized Cu(I) and Ag(I) complexes by condensation of copper(I) or silver(I) halides with indole-3-thiosemicarbazone (Hintsc, **L2**) or 5-methoxy indole-3-thiosemicarbazone (5-MeOHintsc, **L4**) or 5-methoxy indole-N^1-methyl-3-thiosemicarbazone (5-MeOHintsc-N^1-Me, **L5**) (Scheme 3). According to the obtained characterization results, the complexes showed a monomeric tetrahedral structure $[MX(HL)(Ph_3P)_2]$ (in case of M = Cu, **L2**, X = I, **2**; Br, **3**; Cl, **4**; **L4**, X = I, **5**; Br, **6**; Cl, **7**; **L5**, X = I, **8**; Br, **9**; Cl, **10** and in case of M = Ag, **L2**, X = Cl, **14**; Br, **15**; **L3**, X = Cl, **16**, Br, **17**; **L4**, X = Cl, **18**, Br, **19**). Furthermore, the reaction of copper(I) halides with indole-N^1-methyl-3-thiosemicarbazone (HIntsc-N^1-Me, **L3**) resulted in the formation of dinuclear complexes; $[Cu_2(\mu\text{-}X)_2(\eta 1\text{-}S\text{-}H^3L)_2(Ph_3P)_2]$ (X = I, **11**; Br, **12**; Cl, **13**). The characterization of **L3**, **4**, **8**, **9**, **11**, **12** and **14** was carried out by means of single-crystal X-ray diffraction (Figure 5), indicating that the metal ions in the complexes **4**, **8**, **9** and **14** were occupied by one halogen atom, two phosphorous atoms from two triphenylphosphine molecules and a thione sulfur atom from the thiosemicarbazone ligand. However, a halogen bridge connected two copper atoms in complexes **11** and **12**, forming a $(Cu_2(\mu 2\text{-}X)_2Cu$ X = I, **11**; Br, **12**) core. A sulfur atom from the thiosemicarbazone ligand and a phosphorous atom of the triphenylphosphine molecule also coordinated to each copper atom in a trans-position. The authors reported the evaluation of the anti- M. tuberculosis activity of ligands (**L2-L5**) and their metal complexes (**2–19**) against M. tuberculosis H37RV strain ATCC 27294 in which they obtained significant outcomes (MIC = 1.6 μg/ml; much higher than first and second lines drugs employed as positive controls) for the ligand **L4**, Cu(I) complexes **2** and **3**, and Ag(I) complex **14** [48].

Preprints (www.preprints.org) | NOT PEER-REVIEWED | Posted: 20 December 2023 doi:10.20944/preprints202312.1571.v1

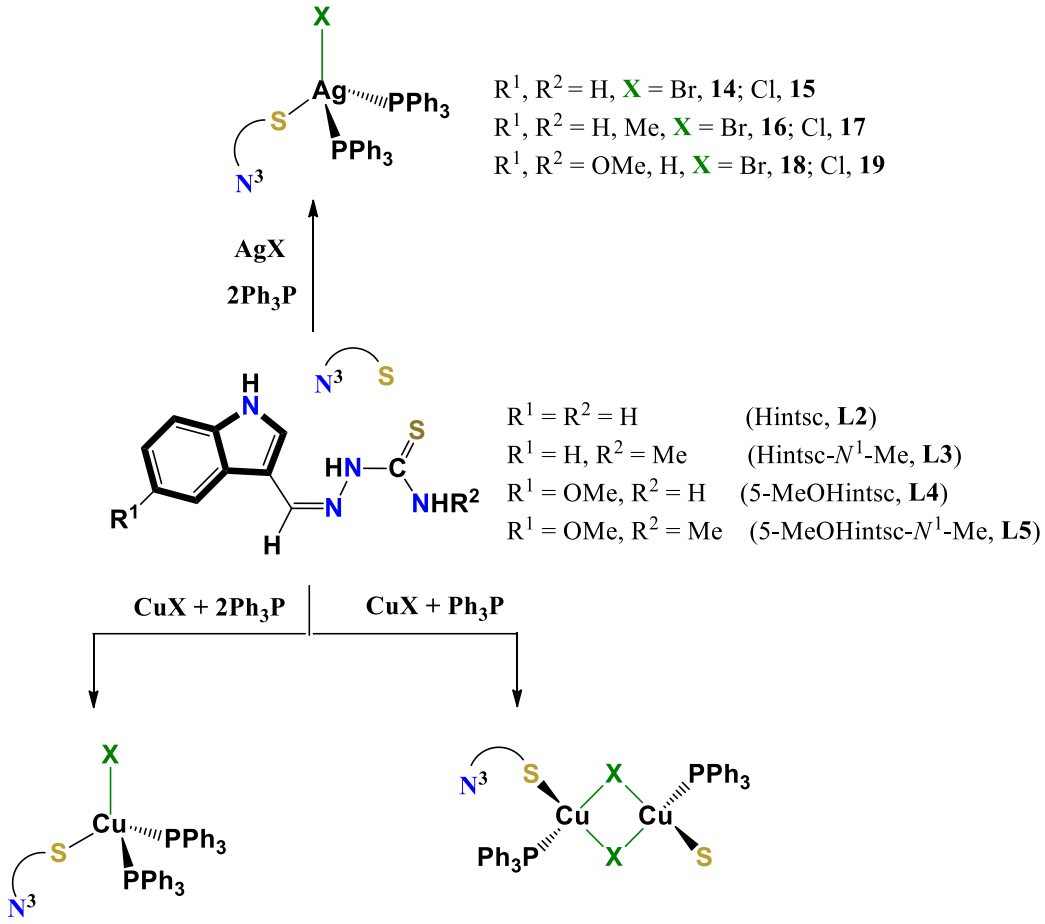

R^1, R^2 = H, **X** = Br, **14**; Cl, **15**
R^1, R^2 = H, Me, **X** = Br, **16**; Cl, **17**
R^1, R^2 = OMe, H, **X** = Br, **18**; Cl, **19**

$R^1 = R^2 = H$ (Hintsc, **L2**)
R^1 = H, R^2 = Me (Hintsc-N^1-Me, **L3**)
R^1 = OMe, R^2 = H (5-MeOHintsc, **L4**)
R^1 = OMe, R^2 = Me (5-MeOHintsc-N^1-Me, **L5**)

R^1, R^2 = H, **X** = I, **2**; Br, **3**; Cl, **4**
R^1, R^2 = OMe, H, **X** = I, **5**; Br, **6**; Cl, **7**
R^1, R^2 = OMe, Me, **X** = I, **8**; Br, **9**; Cl, **10**

R^1, R^2 = H, Me, **X** = I, **11**; Br, **12**; Cl, **13**

Scheme 3. Synthesis of the indole complexes of Cu(I) and Ag(I) **2-19** from ligands **L2-L5**.

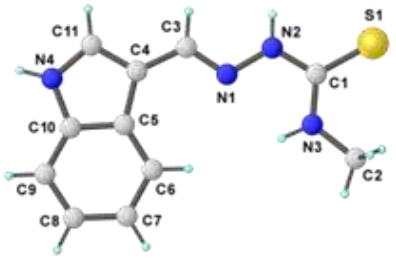

L3

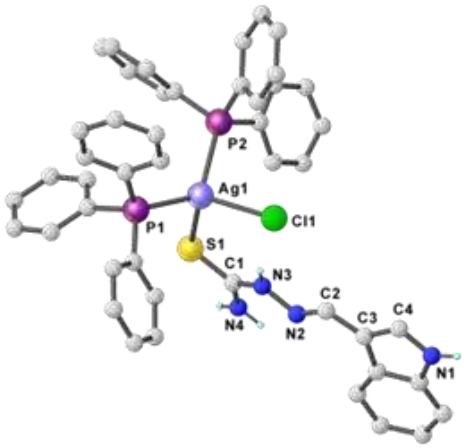

4

Preprints (www.preprints.org) | NOT PEER-REVIEWED | Posted: 20 December 2023 doi:10.20944/preprints202312.1571.v1

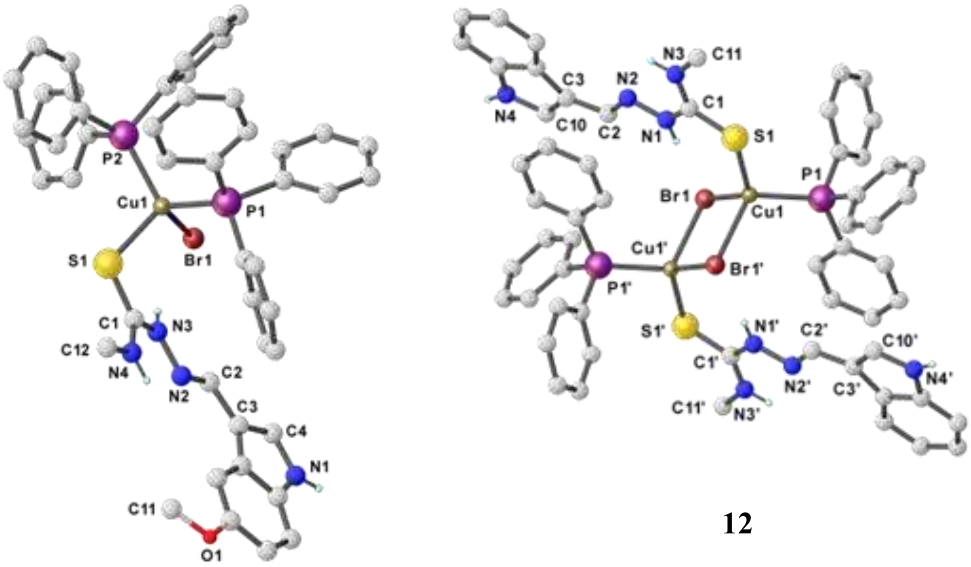

9 **12**

Figure 5. Crystal structure of the ligand **L3** and complexes **4**, **9** and **12**.

3. Bidentate ligands

3.1. O, O-donor

In 2014, Asha Chilwal and co-workers synthesized six organotin(IV) complexes of Me_2SnL_2, Bu_2SnL_2, and Ph_3SnL [where L = indole-3-butyric acid (IBH; i.e. **20, 21** and **22** in Figure 6) or indole-3-propionic acid (IPH; i.e. **23**, **24** and **25** in Figure 6)] by reaction of the corresponding di-organotin(IV) oxide and triphenyltin(IV) hydroxide IBH or IPH in the desired molar ratios of 1:2/1:1 [49]. The characterization of all compounds has been carried out by means of elemental analysis, thermogravimetry (TG) technique, IR, ^{1}H NMR, ^{13}C NMR, and ^{119}Sn NMR spectroscopy. The structures of the complexes were suggested based on the magnitudes of the coupling constants $1J(^{119}Sn–^{13}C)$, namely a tetrahedral geometry around the tin atom in solution for the tri-organotin complexes (**22** and **25**) and an octahedral geometry in solution as well as in the solid state for the di-organotin(IV) complexes (**20**, **21**, **23**, and **24**) (Figure 6). In addition, the authors studied the effects of the metal complexes on three gram-positive (Staphylococcus aureus, Staphylococcus epidermidis, and Micrococcus luteus) and three gram-negative (Escherichia coli, Pseudomonas aeruginosa, and Enterobacter aerogenes) bacteria using the minimum inhibition concentration (MIC) method. Several important results have been achieved: 1) the synthesized compounds were more active against gram-positive than gram-negative bacteria; 2) upon complexation, the antimicrobial activity was remarkably enhanced realistically due to enhanced lipophilicity; 3) the synthesized compounds exhibited greater antibacterial activity as compared to the reference drug (chloramphenicol).

Preprints (www.preprints.org) | NOT PEER-REVIEWED | Posted: 20 December 2023 doi:10.20944/preprints202312.1571.v1

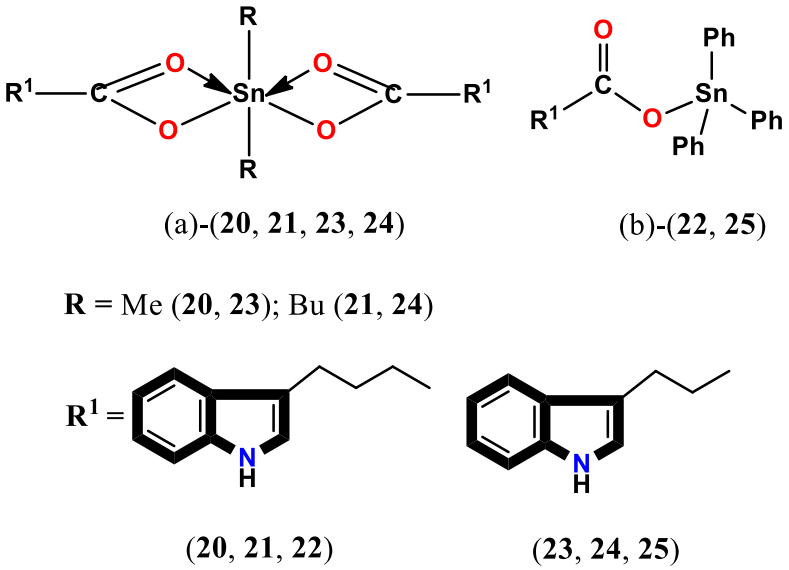

Figure 6. Suggested chemical structure of the complexes **20–25**: (a) octahedral geometry; (b) tetrahedral geometry.

3.2. N, N-donor

The reaction of the 2-imino-indole derivatives **L6-L11** (which were in turn synthetized by condensation of one equivalent of the appropriate aniline with one equivalent of 3-chloro-1H-indole-2-carboxaldehyde) with trans-chloro(1-naphtyl)bis(triphenylphosphine)nickel(II) [$C_{10}H_7NiCl(PPh_3)_2$] led to a series of neutral nickel complexes (i.e. **26-31**; Scheme 4) [50]. The X-ray study of the complex **31** revealed that the nickel atom adopts a square-planar coordination geometry wherein the 2,4,6-trimethylanil and naphthyl group occupy the position trans to the triphenylphosphine ligand (with a P1–Ni1–N2 angle of 174.56(12)°) and to N1 (with an N1–Ni1–C34 angle of 168.6(3)°), respectively (Figure 7). The cytostatic activity of the complexes was investigated for ethylene oligomerization with no additional activator, displaying significant activity (up to 2.05×10^4 g ethylene mol^{-1} h^{-1}) for each of them according to following order: **30** > **28** > **27** > **29** > **31** > **26** [50].

Preprints (www.preprints.org) | NOT PEER-REVIEWED | Posted: 20 December 2023 doi:10.20944/preprints202312.1571.v1

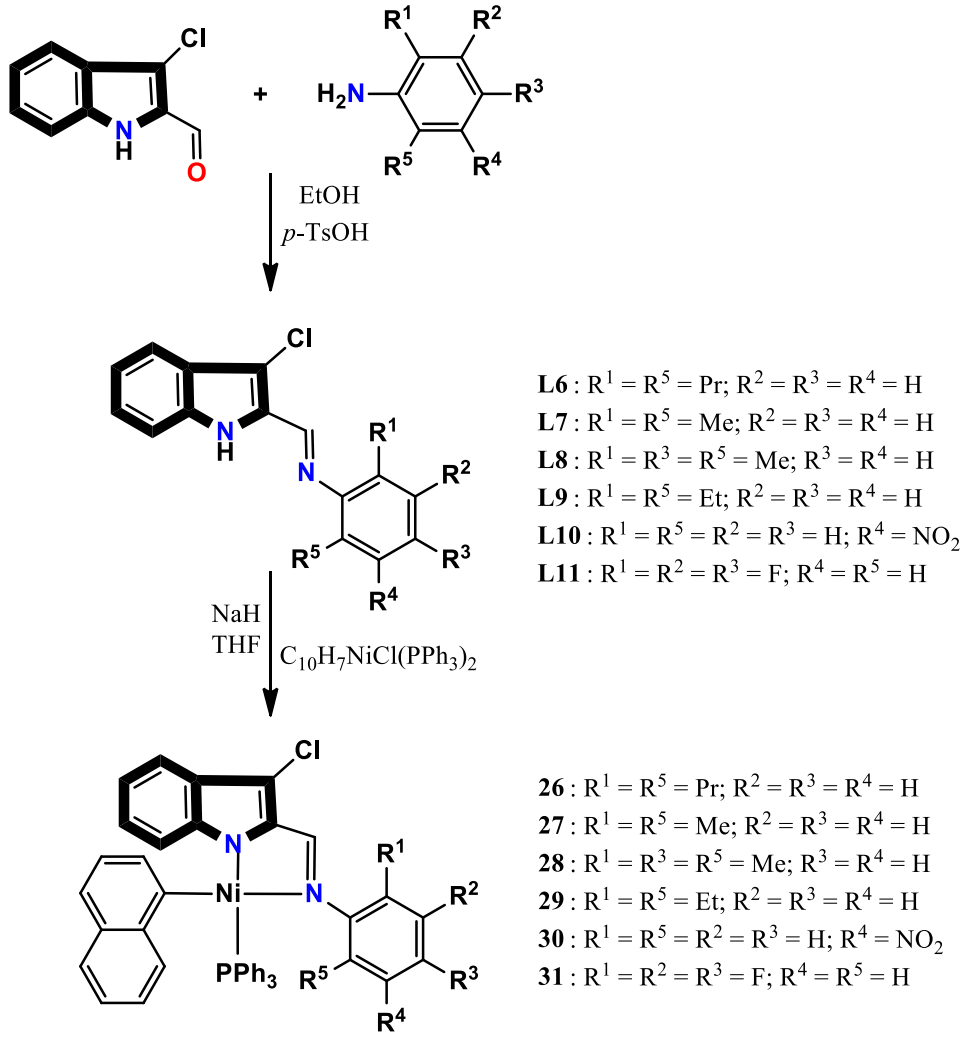

L6 : $R^1 = R^5 = Pr$; $R^2 = R^3 = R^4 = H$
L7 : $R^1 = R^5 = Me$; $R^2 = R^3 = R^4 = H$
L8 : $R^1 = R^3 = R^5 = Me$; $R^3 = R^4 = H$
L9 : $R^1 = R^5 = Et$; $R^2 = R^3 = R^4 = H$
L10 : $R^1 = R^5 = R^2 = R^3 = H$; $R^4 = NO_2$
L11 : $R^1 = R^2 = R^3 = F$; $R^4 = R^5 = H$

26 : $R^1 = R^5 = Pr$; $R^2 = R^3 = R^4 = H$
27 : $R^1 = R^5 = Me$; $R^2 = R^3 = R^4 = H$
28 : $R^1 = R^3 = R^5 = Me$; $R^3 = R^4 = H$
29 : $R^1 = R^5 = Et$; $R^2 = R^3 = R^4 = H$
30 : $R^1 = R^5 = R^2 = R^3 = H$; $R^4 = NO_2$
31 : $R^1 = R^2 = R^3 = F$; $R^4 = R^5 = H$

Scheme 4. Synthesis of the Ni(II) complexes **26-31** from ligands **L6-L11**.

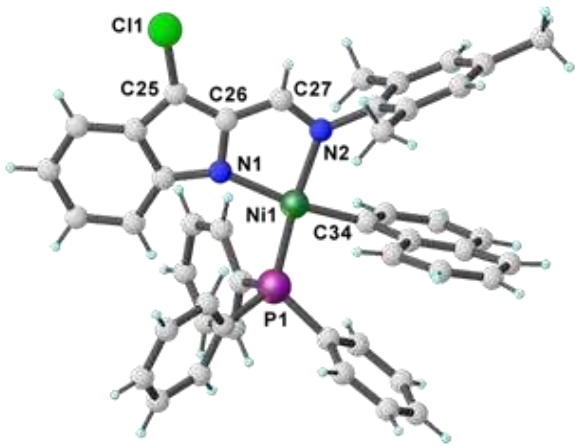

28

Figure 7. Crystal structure of the complex **28**.

Joan J. Soldevila-Barreda and co-workers proposed four half-sandwich complexes containing the 2-(2-pyridinyl)-1H-indole (ind-py) moiety as a ligand (i.e. **32–35**; Figure 8) [51], which were characterized by ^{1}H and ^{13}C-NMR spectroscopy and high-resolution ESI-MS. To evaluate their antiproliferative activity the authors performed the MTT assay by using two ovarian cancer cell lines

Preprints (www.preprints.org) | NOT PEER-REVIEWED | Posted: 20 December 2023 doi:10.20944/preprints202312.1571.v1

(cisplatin sensitive A2780 and cisplatin resistant A2780cisR) and one normal prostate cell line (PNT2). This assay evidenced that the cytotoxicity of the complexes was overall lower than that of the reference drug cisplatin (range 13.0–62.8 μM). Noteworthy, the cytotoxic activity of the Rh(III) (**32**) and Os(II) (**35**) complexes was 2–3 folds higher towards A2780 with respect to normal cells. In addition to this, the authors investigated the catalytic activity of the compounds for reduction/oxidation of nicotinamide adenine dinucleotide coenzymes (NAD) through NMR spectroscopy. Based on the results obtained, the reduction of NAD+ occurred with all complexes and in the presence of sodium formate with turnover frequencies comparable to those of previously reported catalytic metallodrug candidates. They also employed the co-incubation method with sodium formate and N-acetyl cysteine to study the in-cells catalytic activity of the complexes, concluding that only the Ir(III) (**33**) and Rh(III) (**32**) complexes are able to generate oxidative stress [51].

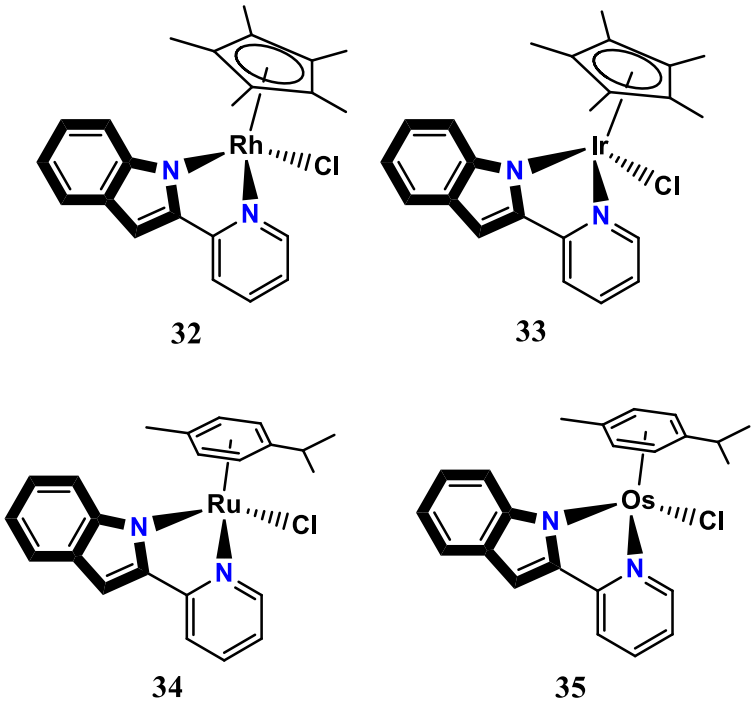

Figure 8. Chemical structure of the complexes **32–35**.

Six Zn(II) complexes (i.e. **36-41**; Scheme 5) with formula [Zn(InR-Im)$_2$Cl$_2$], where InIm is 3-((1H-imidazol-1-yl)methyl)-1H-indole, were designed and synthesized from their corresponding ligands (**L7-L12**; Scheme 5) by K. Babijczuk and co-workers [52]. The investigation of their structures was accomplished through NMR, FT–IR and ESI–MS spectrometry, elemental analysis and single-crystal X-ray diffraction. According to the data obtained, complexes **36**, **37**, **38**, **39** and **40** are composed of a zinc ion coordinated by two imidazole nitrogen atoms of two indole–imidazole hybrid ligands and two chloride ions in a distorted tetrahedral environment. The crystal structure of complex **39** is shown in Figure 9 as an example of the determined similar structures. The comparison between the structure of the complex **38** and its uncoordinated ligand **L9** revealed that the absolute values of the torsion angles along the C–C (φ1) and C–N (φ2) bonds formed by the methylene bridge increases and decreases upon complexation, whereas these conformational changes are not significant in the case of the complex **40**. Hemolytic activity assays showed that only the complexes with electron-withdrawing groups in the imidazole ring (i.e. **40** and **41**) are notably cytotoxic (> 5%) as compared to the free ligands. On the contrary, the complexes containing either an unsubstituted or electron-donor-substituted ligand at the same nucleus showed no toxicity. The cytoprotective activity of the complexes against AAPH-induced hemolysis was also studied indicating that this activity increases upon complexation with $ZnCl_2$ following the order **36** > **39** > **37** > **40** > **41** > **38**. Furthermore, these

Preprints (www.preprints.org) | NOT PEER-REVIEWED | Posted: 20 December 2023 doi:10.20944/preprints202312.1571.v1

complexes turned out to be effective as antibacterial (in particular **36** against Micrococcus luteus; growth inhibition zone = 10.6 mm) and antifungal (in particular **41** against fungi of the genus Trichoderma) agents [52].

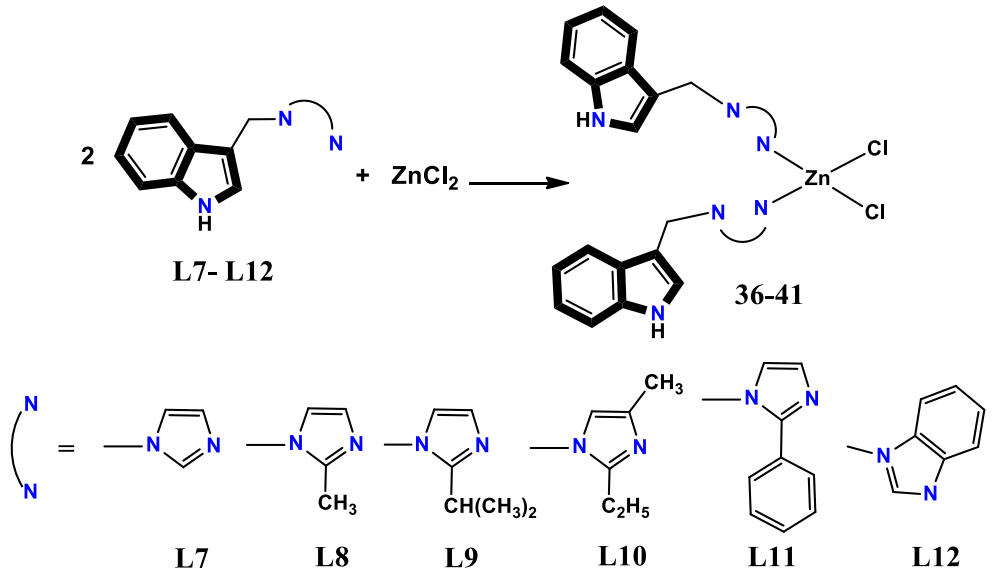

Scheme 5. Synthesis of the complexes **36–41** from ligands **L7–L12**.

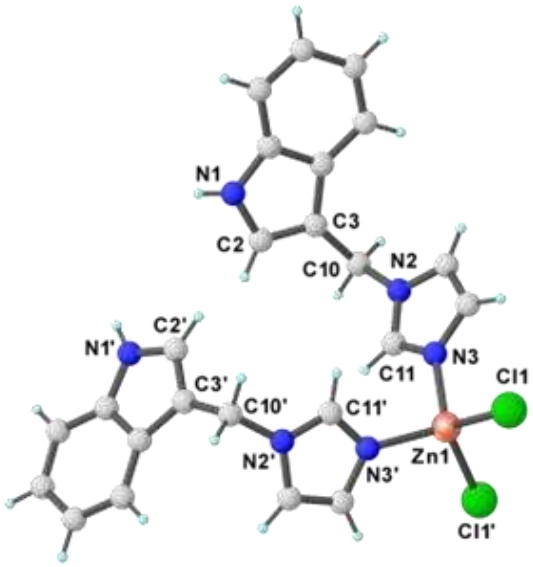

39

Figure 9. Crystal structure of the complex **39**.

A series of luminescent rhenium(I) diimine indole complexes (i.e. **42a-45b**; Figure 10) and their indole-free counterparts (**42c-45c**; Figure 10) were obtained by K. Kam-Wing Lo et al. in 2005 by using py-3-CONHC$_2$H$_4$-indole, py-3-CONHC$_5$H$_{10}$CONHC$_2$H$_4$-indole, or py-3-CONH-Et ligands as N donor in combination with diamine ligands, i.e. Me$_4$-phen, phen, Me$_2$-phen and Ph$_2$-phen [53]. According to X-ray analysis, in the crystal structure of **44a** the Re(I) center adopted a distorted octahedral geometry and coordinated with two carbonyl groups in a facial orientation, while a dihedral angle of ca. 7.29° was formed from the indole unit and the Me$_2$-phen ligand of the same molecule (Figure 11). In this complex no stacking interactions were observed between the diimine ligand and the indole moiety of adjacent molecules. All newly synthesized complexes showed green to orange-yellow luminescence upon visible-light excitation. The indole-containing complexes'

Preprints (www.preprints.org) | NOT PEER-REVIEWED | Posted: 20 December 2023 doi:10.20944/preprints202312.1571.v1

spectra recorded in the ultraviolet region produced an additional emission band due to the indole moiety. The lower luminescence intensity of the complex compared to free indole is probably due to strong absorbance of rhenium(I)-diimine units at the excitation wavelength or resonance energy transfer from the indole to the luminophore. To gain insight into the quenching mechanism, Stern-Volmer studies on the indole-free complexes in the presence of indole as a quencher were performed. These additional studies confirmed the self-quenching of the indole-containing complexes which stem from the intermolecular electron transfer. Moreover, the emission titration technique was employed to evaluate the bovine serum albumin (BSA)-binding of the diamine-indole complexes. This binding study clearly indicated that the indole moiety is responsible for the protein-complex formation since no binding to BSA was observed in the indole-free complexes. This set of rhenium(I) diamine-indole complexes was also investigated for their ability to inhibit the bacterial enzyme Tryptophanase (TPase). Also in this case, the binding of the complexes to the enzymatic protein (and the consequent inactivation) occurs due to the presence of the indole moiety [53].

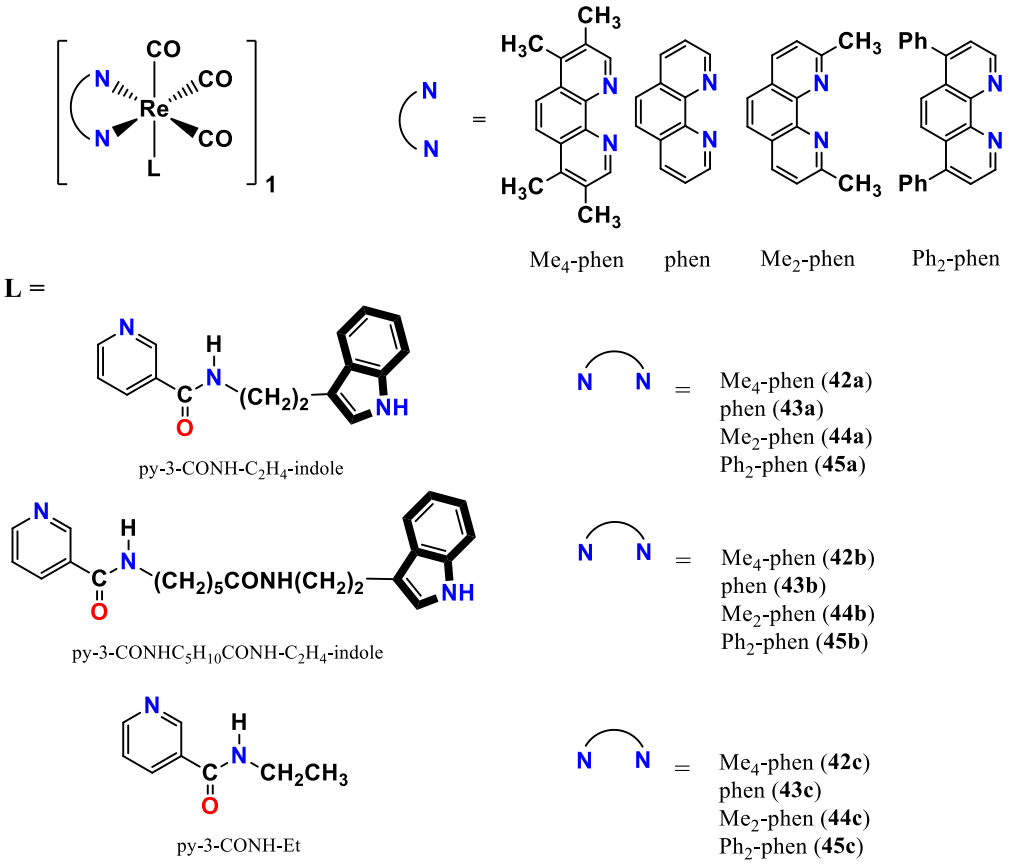

Figure 10. Chemical structure of the rhenium(I) diimine indole complexes **42a–45c** and their ligands.

Preprints (www.preprints.org) | NOT PEER-REVIEWED | Posted: 20 December 2023 doi:10.20944/preprints202312.1571.v1

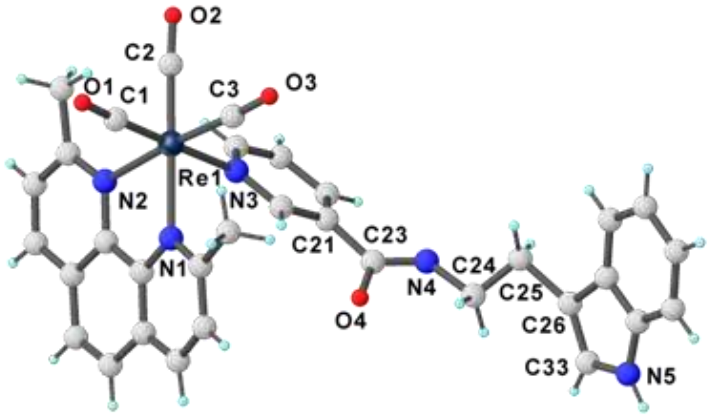

44a

Figure 11. Crystal structure of the complex **44a**.

Synthesis and study of the anticancer activity of novel indole-fused latonduine derivatives and their Ru^{II} and Os^{II} complexes (i.e. **L13-L14** and **46-49**, respectively; Figure 12) were reported by Christopher Wittmann et al. in 2022 [54]. All complexes were found to be chiral at the metal center and as a racemic mixture when in solution. The single-crystal structure of **46** was determined by X-ray diffraction method and revealed that the complex adopted the three-leg piano-stool geometry in which the ruthenium(II) was coordinated to the two N-atoms of the ligand **L13**, one chloride ion and a p-cymene group (Figure 13). Furthermore, the obtained data displayed that the complex crystallizes as a racemate in the orthorhombic space group Pna21 with three-leg piano-stool geometry wherein the bidentate ligand **L13** and a chloride ion act as legs while the p-cymene group was as the piano's stool. Both ligands and complexes were evaluated for their anticancer activity against MDA-MB-231, LM3 and U-87 MG cell lines. The Ru(II) and Os(II) complexes showed a lower efficacy (IC_{50} = 57–250 μM) compared to indole-based ligands (IC_{50} = 1.4–10 μM) and the reference drugs cisplatin, sorafenib and paclitaxel [54].

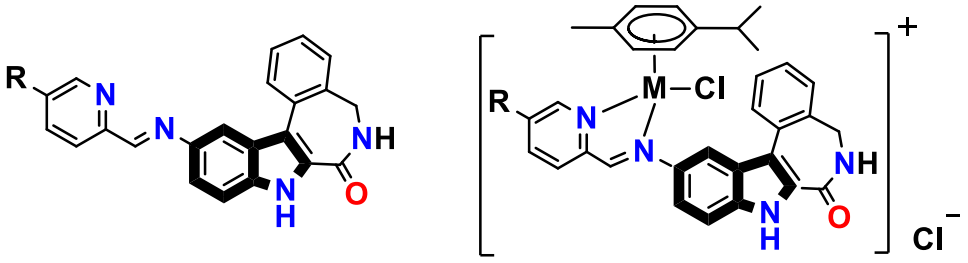

R = H	**L13**
R = *N*-Methylmorpholine	**L14**

M = Ru(II), R = H	**46**
M = Os(II), R = H	**47**
M = Ru(II), R = *N*-Methylmorpholine	**48**
M = Os(II), R = *N*-Methylmorpholine	**49**

Figure 12. Chemical structure of the ligands **L13–L14** and complexes **46–49**.

Preprints (www.preprints.org) | NOT PEER-REVIEWED | Posted: 20 December 2023 doi:10.20944/preprints202312.1571.v1

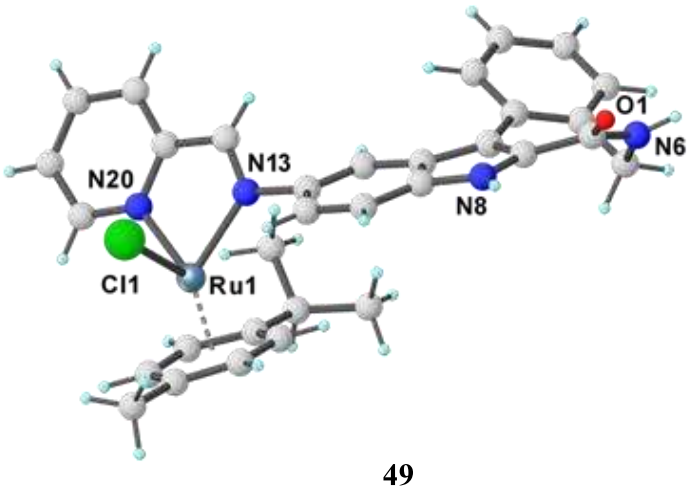

49

Figure 13. Crystal structure of the complex **49**.

A comprehensive study on metal complexes that have an indole derivative as a bidentate ligand has been conducted by Yareeb J. Sahar et al. [55]. By using (E)-2-(1H-indol-3yl)diazenyl)thiazole (HIDAT) ligand (i.e. **L15**; Figure 14) as a starting material, four novel complexes (cobalt, nickel, copper and palladium derivatives) (i.e. **50-53**; Figure 14) were obtained and characterized by means of different techniques. Based on the obtained data, the metal ions in the complexes exhibited an octahedral geometry except for Pd(II) which was square-planar. The Pd(II) complex **50** showed significant anticancer activity against the human leukemia cell line HL-60 (IC_{50} = 27.02 μg/mL) and moderate tumor selectivity evaluated towards HdFn healthy cells (IC_{50} = 83.69 μg/mL). Docking studies were performed to evaluate the interaction between this Pd(II) complex and the tyrosine-protein kinase ABL1 receptor, which is related to the emergence of leukemia according to recent studies [56]. In Figure 15 are displayed in 2D the main interactions **50**-target. The data obtained from these computational studies pertaining the Pd(II) complex and the activity-related reference antineoplastic drug Nelarabine indicated that **50** possesses promising anti-leukemic activity. The high propensity of the complex to bind to the receptor may be due to the presence of the nitrogen and sulfur atoms of the heterocyclic indole and thiazole rings, respectively, in the structure of the complex [55].

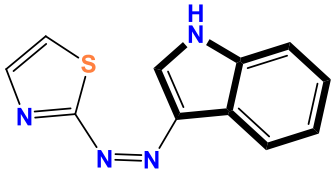

((*E*)-2-((1*H*-indol-3yl)diazenyl)thiazole)(HIDAT)

L15

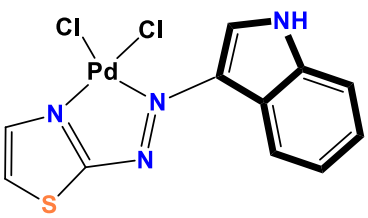

50

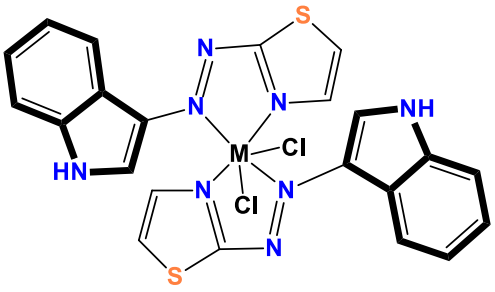

M = Co (**51**); Ni (**52**); Cu (**53**)

Preprints (www.preprints.org) | NOT PEER-REVIEWED | Posted: 20 December 2023 doi:10.20944/preprints202312.1571.v1

Figure 14. Chemical structure of the ligand **L15** and complexes **50-53**.

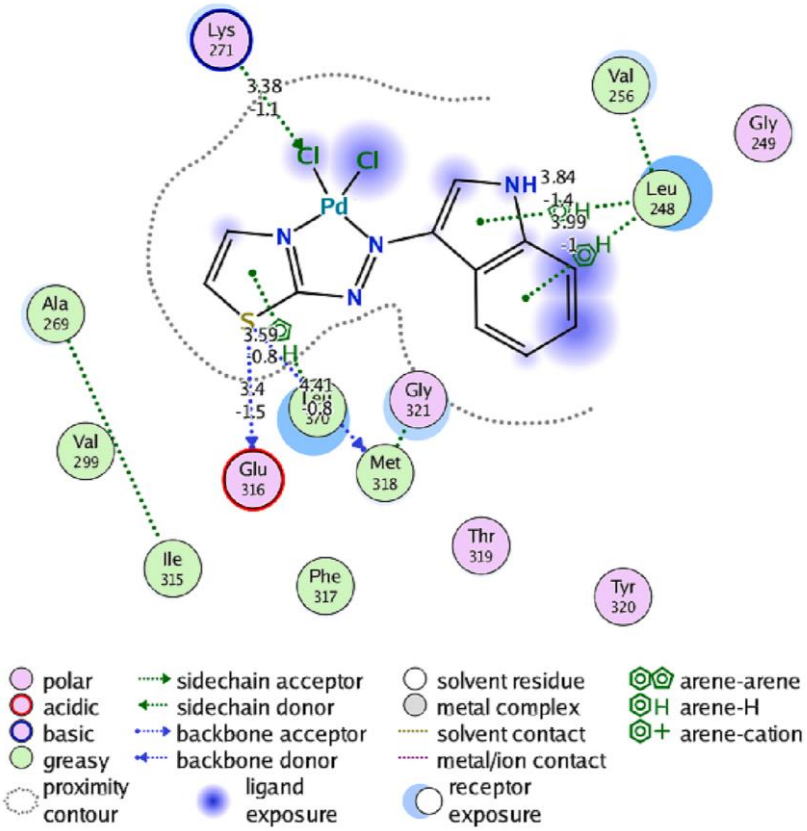

Figure 15. 2D interactions between the Pd(II)-HIDAT complex (**50**) and tyrosine-protein kinase ABL1 receptor.

The 3-methoxy-indole-hydrazone glyoxime ligand **L16** (Figure 16) was used for the preparation of the related Ni(II), Cu(II), and Co(II) complexes (**54**-**56**; Figure 16) and also its BF_2^+-bridged transition metal complexes (**57**-**59**; Figure 16) by Babahan I. et al. [57]. The latter were synthesized through the addition of boron trifluoride etherate complex to the solution of $[M(L)_2]$. The Co(II) complex **56** showed an octahedral geometry with water molecules as axial ligands while a square planar environment was suggested for the Ni(II) and Cu(II) complexes (**54** and **55**, respectively), highlighting the effect of metal ions on the complexes' structures. Based on the spectral studies, the ligand acted as a neutral bidentate N, O-donor through the azomethine nitrogen atom and the imine oxime group. The antitumor potential of these complexes was evaluated against MCF-7 and PC-3 cell lines. Additionally, the Hoechst/propidium iodide double staining method was employed to determine their apoptotic or necrotic effects towards cells. From these biological assessments emerged that all compounds were effective against both tumor cell lines in the range of 5–40 μM suggesting apoptotic mechanisms. More importantly, it turned out that their cytotoxic activity was higher than that of the already approved anticancer drug paclitaxel used as a positive control [57].

Preprints (www.preprints.org) | NOT PEER-REVIEWED | Posted: 20 December 2023 doi:10.20944/preprints202312.1571.v1

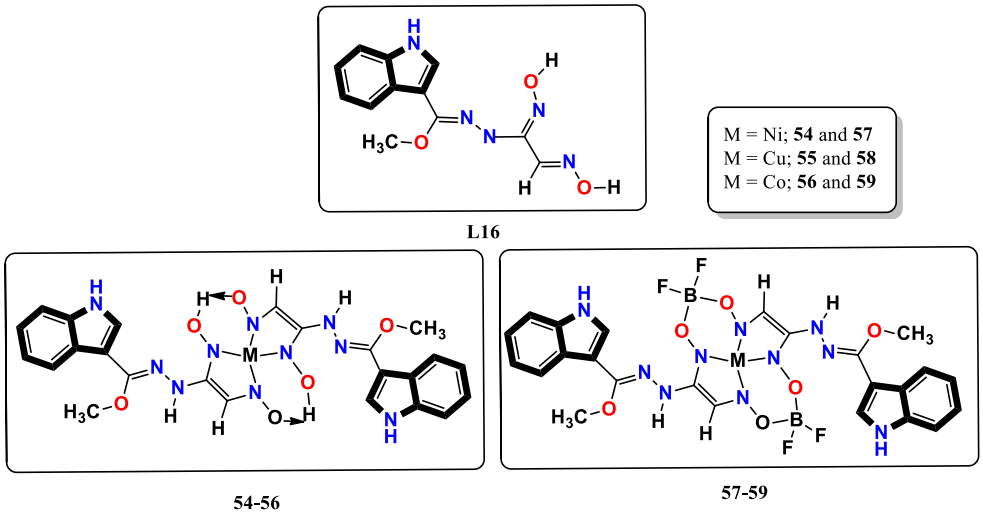

Figure 16. Chemical structure of the ligand **L16** and complexes **54-59**.

3.3. N, O-donor

Novel Ni(II) (**60** and **62**; Figure 17) and Cu(II) complexes (**61** and **63**; Figure 17) have been prepared from the Schiff base ligand **L17** ((E)–2–(((5H–[1,2,4]triazino[5,6–b]indol–3–yl)imino)methyl)phenol), which was in turn synthesized by condensation of 5H-[1,2,4]triazino[5,6-b]indol-3-amine and a salicylaldehyde unit [58]. The Ni(II) center in **60** and **62** adopted a square planar geometry, unlike **61** and **63** in which an octahedral geometry was observed around the Cu(II) center. Electronic absorption titrations and fluorescence spectral studies displayed an interaction of the complexes with DNA, probably by electrostatic surface binding mode along with partial intercalation in the minor groove mode. K_b values evidenced that the complexes containing phen **62** ($1.9 \times 10^4\ M^{-1}$) and **63** ($4.8 \times 10^4\ M^{-1}$) possess a greater CT-DNA binding capacity than the complexes with bpy **60** and **61**. The two phen derivatives showed also superior HAS-binding capacity compared to the bpy derivatives [58].

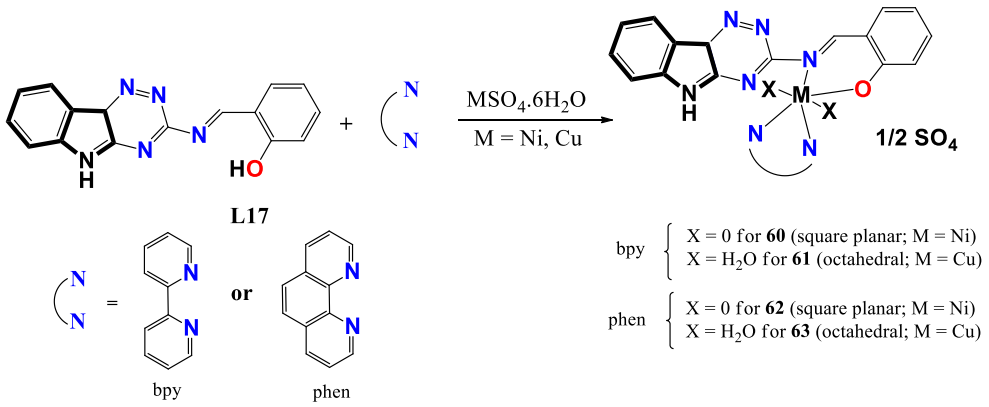

Figure 17. Synthesis of the complexes **60-63** from ligand **L17**.

Two Co(II) and Zn(II) complexes containing an indole ring (i.e. **64** and **65**; Figure 18) with a bidentate ligand has been proposed by Youssef Ghufran Shakir et al.[59]. The reaction of the combined ligand (i.e. **L18**; Figure 18), which was in turn synthetized by condensation of the diazonium salt of 4-aminoantipyrine and indole in basic conditions, with $CoCl_2 \cdot 6H_2O$ and $ZnCl_2$ led to these complexes. ^{1}H-NMR, IR, mass spectrometry, UV-Vis, powdered XRD, molar conductivity and magnetic susceptibility technique were utilized to determine the structure and properties of the ligand and its complexes. The cytostatic activity of the ligand and its complexes was investigated against MCF-7 tumor cell line and HdFn healthy cell line. All the examined compounds displayed higher cytotoxicity against MCF-7 cells than HdFn cells. Particularly, **L18** was more effective against

Preprints (www.preprints.org) | NOT PEER-REVIEWED | Posted: 20 December 2023 doi:10.20944/preprints202312.1571.v1

MCF-7 cells as compared to the zinc complex **65**. Additionally, well diffusion method was employed to investigate the antimicrobial activity of the compounds against Staphylococcus aureus and Escherichia coli bacteria, revealing higher inhibitory properties of the complexes than that of the ligand [59].

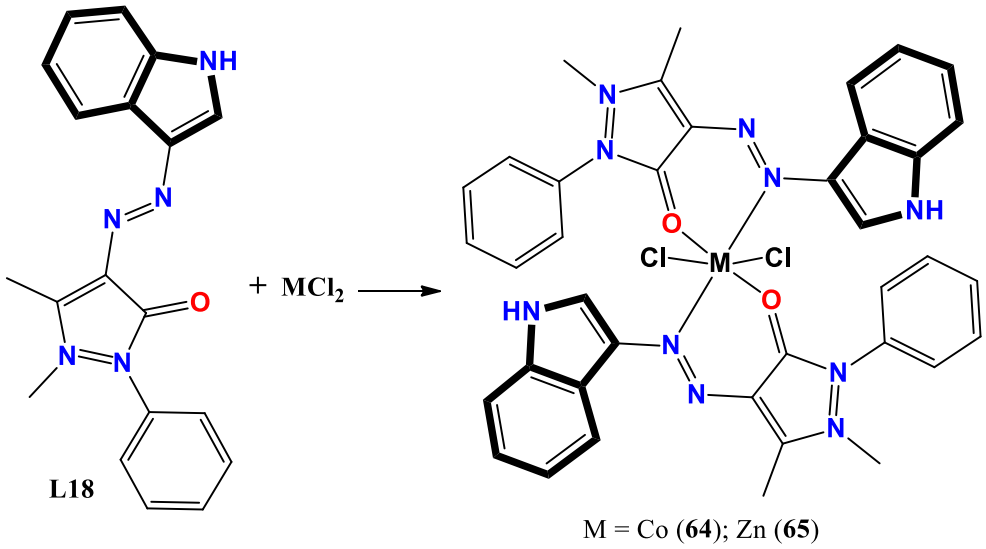

Figure 18. Synthesis of the complexes **64** and **65** from ligand **L18**.

R. Reshma and et al. [60] developed a series of Mn/Fe/Co/Ni/Cu/Zn(II)-(indal-L-his) complexes starting from the ligand **L19** (i.e. **66-71**; Figure 19) [60]. The indole-based ligand was obtained in turn by reaction of the indole-3-carboxaldehyde (indal) with L-histidine (L-his). The structure of all complexes was determined using elemental analysis, molar conductivity, magnetic, IR, UV–Vis, ^{1}H NMR, mass and ESR spectroscopy, powder XRD and thermal gravimetric analysis (TGA). Interestingly, Mn(II) and Fe(II) complexes (**66** and **67**, respectively) adopted an octahedral geometry, [M(II)-(indal-L-his)$_2$(H$_2$O)$_2$], whilst Co(II) and Zn(II) complexes (**68** and **71**, respectively) with [M(II)-(indal-L-his)$_2$] formula possessed a tetrahedral geometry. A square planar environment was observed for Ni(II) and Cu(II) complexes (**69** and **70**, respectively), [M(II)-(indal-L-his)$_2$]. Based on the results of the antimicrobial tests, all metal complexes exhibited higher activity than the indal-L-his ligand **L19** against several Gram-positive and Gram-negative bacteria. The copper derivative **70** ([Cu(II)-(indal-L-his)$_2$]) displayed the most significant activity amongst all complexes. The antimicrobial activity of this copper complex was superior to that of the reference drug ciprofloxacin [60].

Preprints (www.preprints.org) | NOT PEER-REVIEWED | Posted: 20 December 2023 doi:10.20944/preprints202312.1571.v1

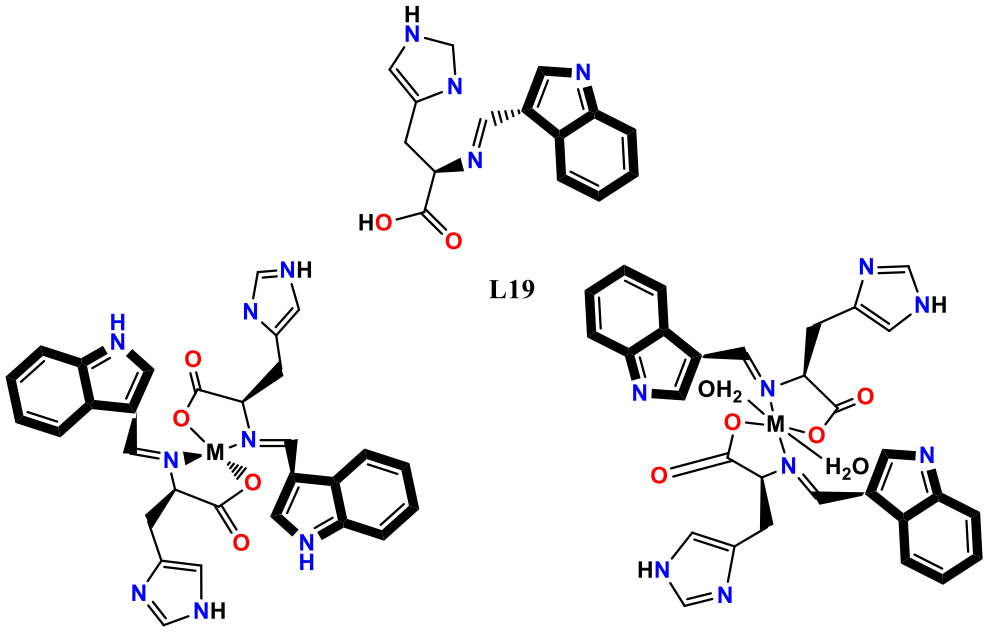

Figure 19. Chemical structure of the ligand **L19** and complexes **66-71**.

Synthesis and characterization of a series of Cu(II), Co(II), Ni(II) and Zn(II) complexes (i.e. **72-79**; Figure 20) containing amino acid-derived Schiff base ligands with general formula [ML_2] (**72-75**) and [ML(1,10-phen)$_2$]Cl (**76-79**) have been achieved by Arunadevi A. & Raman N. [61]. The preparation of the ligand (**L20**) has been carried out by condensation of the 4-chloro-3-nitrobenzaldehyde and 2-amino-3-(1H-indol-3-yl)propanoic acid. This series of complexes were assessed for their antimicrobial (antibacterial and antifungal) activity and binding properties towards biological targets (DNA and BSA). Overall these studies highlighted the higher efficacy of the metal complexes compared to free ligand [61]. **L20** and the whole panel of metal complexes underwent also exhaustive computational studies which highlighted their drug-likeness profile for oral administration and the binding with DNA [62].

Preprints (www.preprints.org) | NOT PEER-REVIEWED | Posted: 20 December 2023 doi:10.20944/preprints202312.1571.v1

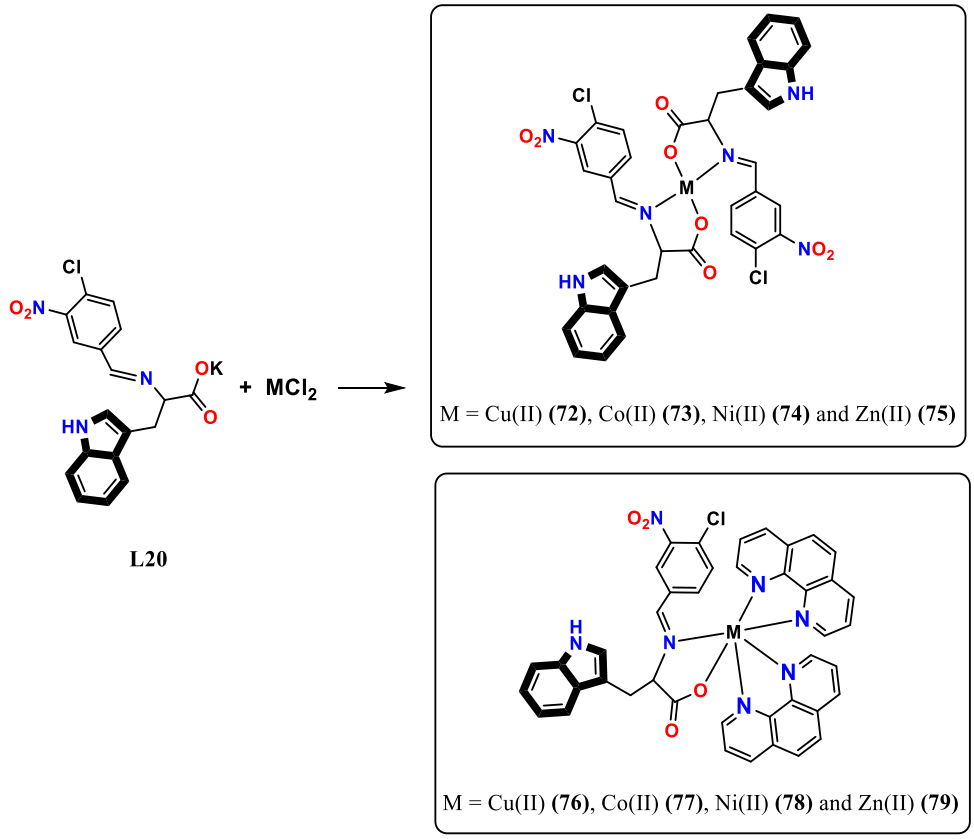

Figure 20. Synthesis of the complexes **72-79** from ligand **L20**.

Synthesis and characterization of mononuclear rhenium(I) complexes (i.e. **80-84**, Figure 21) with bidentate indole-pyrazoline based ligands (i.e. **L21-L25**, Figure 21) derived from α,β unsaturated enons and benzhydrazide have been reported by Reena R. Varma et al. [63]. The DNA-binding, in vivo and in vitro cytotoxicity as well as the antimicrobial activity of the complexes and ligands have been investigated. The results suggested DNA groove binding mode for all compounds with affinity in the order **84** > **80** > **83** > 81 > **82** > **L25** > **L21** > **L22** > **L23** > **L24**. All complexes also exhibited good antiproliferative activity against MCF-7, HCT 116, and A549 tumor cell lines. In particular, complex **84** showed the highest cytotoxicity (higher also than that of the anticancer drugs carboplatin and oxaliplatin used as positive controls [63].

Preprints (www.preprints.org) | NOT PEER-REVIEWED | Posted: 20 December 2023 doi:10.20944/preprints202312.1571.v1

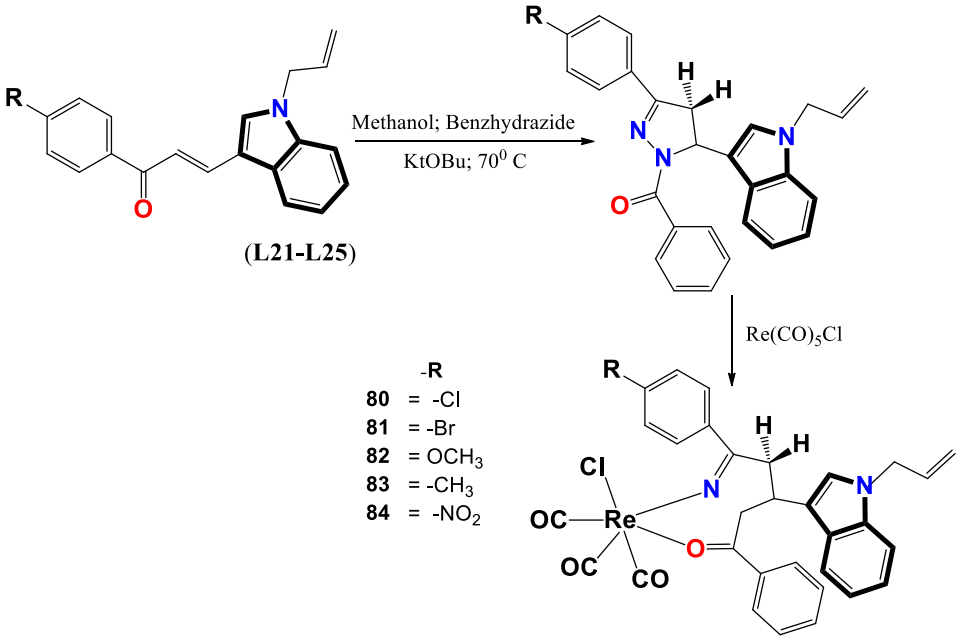

Figure 21. Synthesis of the complexes **80-84** from ligands **L21-L25**.

Further advancements in the development of metal complexes endowed with indole rings in the structure of the ligand and containing manganese(II) as a transition metal were reported by S. Sharma et al. in 2016 [64]. In this research work, four bidentate ligands were synthesized, namely **L26** [2-(5-fluoro-2-dihydro-2-oxo-1H-indol-3-ylidene)hydrazinecarboxamide], **L27** [2-(5-fluoro-2-dihydro-2-oxo-1H-indol-3-ylidene)hydrazinecarbothioamide], **L28** [2-(5-bromo-2-dihydro-2-oxo-1H-indol-3-ylidene)hydrazinecarboxamide] and **L29** [2-(5-bromo-2-dihydro-2-oxo-1H-indol-3-ylidene)hydrazinecarbothioamide] (Figure 22). Their complexation with $MnCl_2 \cdot 4H_2O$ led to Mn(II) complexes (i.e. **85-92**; Figure 22) which, based on the spectral data, showed a tetrahedral geometry. Both the ligands and complexes showed acceptable toxicity against bacteria (Escherichia coli and Staphylococcus aureus) and fungi (Fusarium semitectum and Aspergillus flavus), with the complexes being more active than the ligands. Coordination of metal ions correlates with enhancement of DNA-cleavage activity by the complexes, as demonstrated by gel electrophoresis experiments. Specifically, thiosemicarbazone complexes **86** and **90** exhibited better DNA-cleavage activity than the corresponding semicarbazone derivatives **85** and **89** [64].

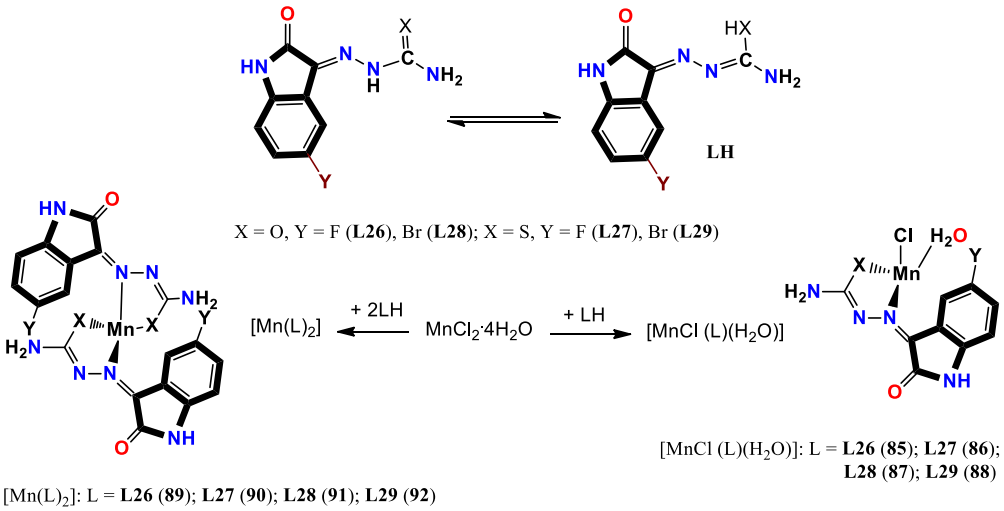

Figure 22. Synthesis of the complexes **85-92** from ligands **L26-L29**.

Preprints (www.preprints.org) | NOT PEER-REVIEWED | Posted: 20 December 2023 doi:10.20944/preprints202312.1571.v1

Co(II) and Ni(II) complexes (i.e. **93-94**; Figure 23) were obtained by I. I. Seifullina and co-workers in 2020 via the reaction of $M(CH_3COO)_2$ with 2-(7-bromo-2-oxo-5-phenyl-3H-1,4-benzodiazepin-1-yl)acetohydrazide (Hydr) and an indole derivative, i.e. 1H-indole-2,3-dione (HIz). The structure of the complexes was investigated using elemental analysis, thermogravimetry, IR spectroscopy, mass spectrometry and X-ray absorption spectroscopy. The results suggested an octahedral geometry surrounding the cobalt and nickel ions and composed of six oxygen and nitrogen atoms [65].

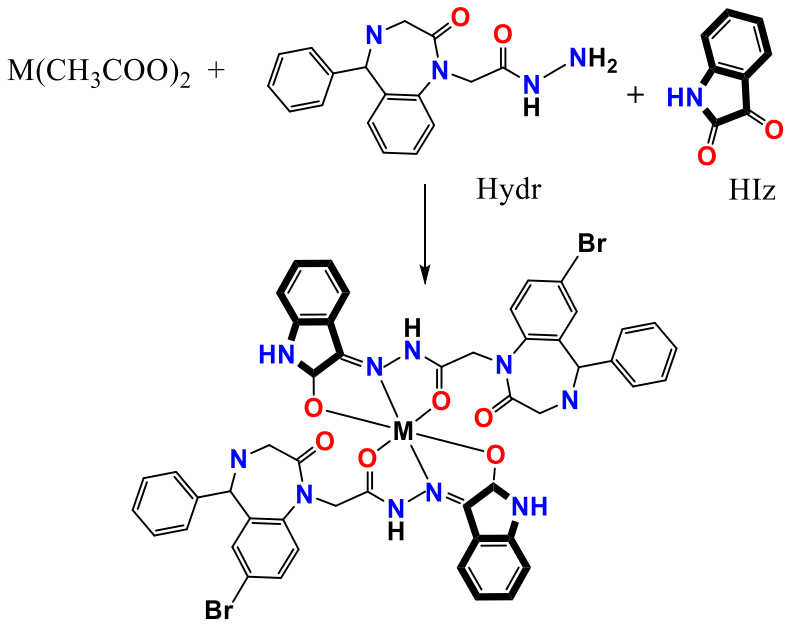

Figure 23. Synthesis of the complexes **93** and **94**.

The tridentate Schiff base ligands **L30–L33** (Figure 24), which were obtained by reaction of indole-3-butyric hydrazide with variously substituted salicylaldehydes, were used for the preparation of diorganotin (IV) complexes, R_2SnL (i.e. **95-110**; Figure 24). The structure of the complexes was determined by using UV–Vis, FT-IR, NMR (^1H, ^{13}C, ^{119}Sn), mass spectrometry and TGA which showed that the metal ions of the dialkyl/diaryltin (IV) moieties were coordinated to two oxygen and one nitrogen atoms of the ligand in a pentacoordinated geometry [66].

Preprints (www.preprints.org) | NOT PEER-REVIEWED | Posted: 20 December 2023 doi:10.20944/preprints202312.1571.v1

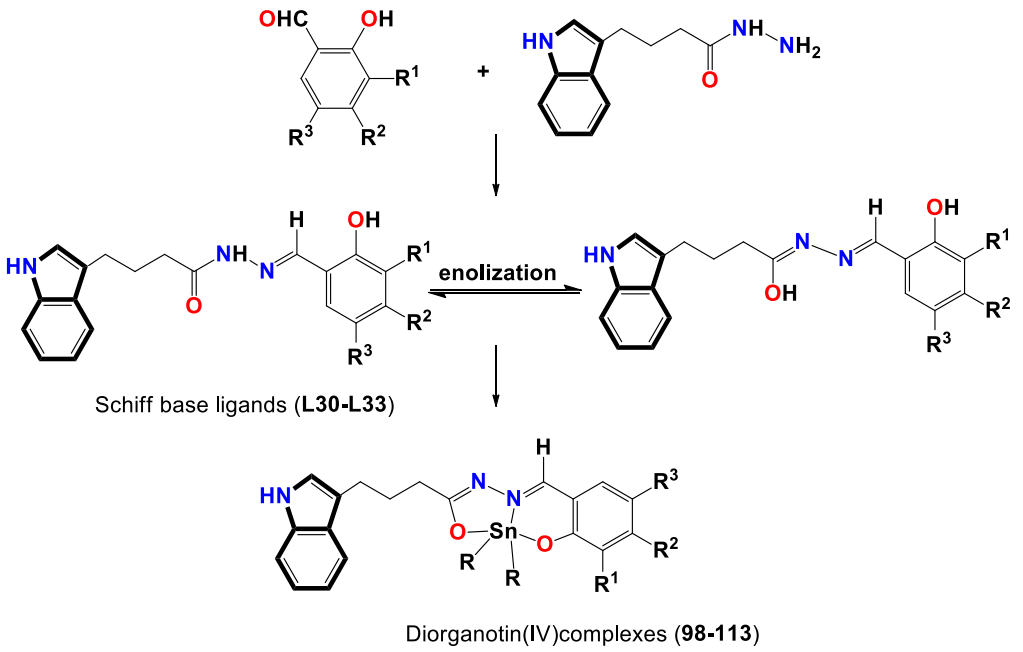

	R_1	R_2	R_3
(**L30**)	H	H	H
(**L31**)	H	H	NO_2
(**L32**)	H	$N(C_2H_5)_2$	H
(**L33**)	Br	H	Br

	R_1	R_2	R_3	R
(**95**)	H	H	H	Me
(**96**)	H	H	H	Et
(**97**)	H	H	H	Bu
(**98**)	H	H	H	Ph
(**99**)	H	H	NO_2	Me
(**100**)	H	H	NO_2	Et
(**101**)	H	H	O_2	Bu
(**102**)	H	H	NO_2	RPh
(**103**)	H	$N(C_2H_5)_2$	H	Me
(**104**)	H	$N(C_2H_5)_2$	H	Et
(**105**)	H	$N(C_2H_5)_2$	H	Bu
(**106**)	H	$N(C_2H_5)_2$	H	Ph
(**107**)	Br	H	Br	Me
(**108**)	Br	H	Br	Et
(**109**)	Br	H	Br	Bu
(**110**)	Br	H	Br	Ph

Figure 24. Synthesis of the complexes **98-113** from ligands **L30-L33**.

3.4. N, N-donor

In order to investigate photophysical and electrochemical properties of indole-based metal complexes, Jason Shing-Yip Lau et al. have synthetized luminescent cyclometalated iridium(III) polypyridine derivatives with general formula ($[Ir(N^{\wedge}C)_2(N^{\wedge}N)](PF_6)$ (i.e. **111-113**; Figure 25) by reaction of $[Ir_2(N^{\wedge}C)_4Cl_2]$ ($HN^{\wedge}C$) Hppy, Hbzq, or Hpq with 2 equivalents of ligand bpy-ind or bpy-C6-ind (Figure 25) [67]. The complexes have been characterized by means of IR and NMR spectroscopy. Moreover, the electrostatic interaction of the complexes with the indole-binding protein BSA was assessed using emission titrations. According to the obtained data, emission and lifetime extension of the complexes have enhanced upon binding to BSA, due to the increased hydrophobicity and rigidity of the local environments of the complexes. The cytotoxicity of these complexes towards HeLa cells was investigated by flow cytometry and laser-scanning confocal microscopy. These studies highlighted efficient uptake of the complex **113a** by HeLa cells [67].

Preprints (www.preprints.org) | NOT PEER-REVIEWED | Posted: 20 December 2023 doi:10.20944/preprints202312.1571.v1

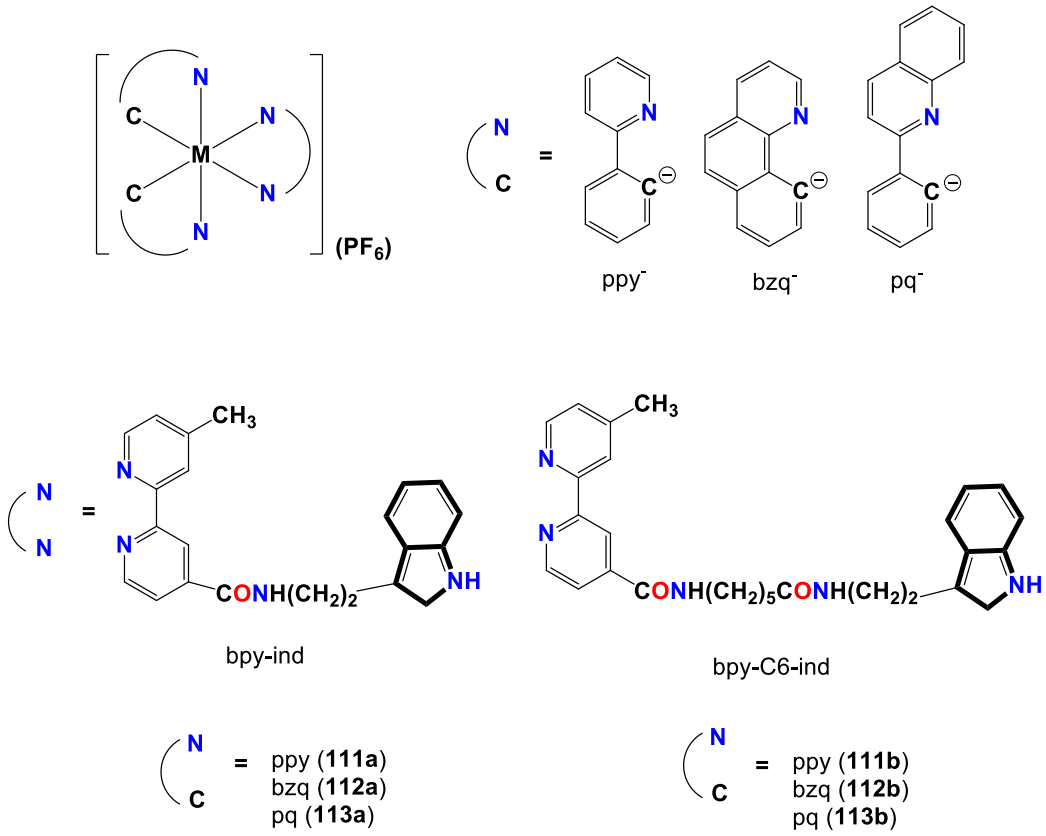

Figure 25. Chemical structure of the complexes **111a-113b** and related ligands.

3.5. N, S-donor

In the research work of Jebiti Haribabu et al., the DNA-binding of the metal complexes has been explored using absorption spectroscopic and ethidium bromide (EB) competitive binding studies [68]. Using indole-based thiosemicarbazone ligands (**L34-L37**; Figure 26) as starting materials, a small set of Ni(II) complexes [Ni{$C_{10}H_9N_2NHCSNH(R)$}$_2$] where R = hydrogen (**114**), 4-methyl (**115**), 4-phenyl (**116**) and 4-cyclohexyl (**117**); Figure 26) were obtained and characterized by elemental analyses, UV–Vis, FT-IR, ^{1}H and ^{13}C NMR and mass spectroscopic techniques. The molecular structure of the ligands **L36** and **L37** and complexes **115**, **116** and **117** has also been confirmed through X-ray diffraction analysis (Figure 27). The investigation of their biological activity revealed the intercalative interaction of the complexes with CT-DNA. Furthermore, based on obtained data by UV–Vis, fluorescence and synchronous fluorescence spectroscopic methods, the compounds displayed strong BSA-interaction. All Ni(II) complexes displayed high antioxidant activity (assessed by DPPH method) and antihaemolytic activity. They also showed moderate to remarkable anticancer activity against lung cancer (A549), human breast cancer (MCF7) and mouse embryonic fibroblasts (L929) cell lines. Complex **117** possessed the highest cytotoxicity assessed using the Hoechst 33258 staining method to analyze the mode of cell death [68].

Preprints (www.preprints.org) | NOT PEER-REVIEWED | Posted: 20 December 2023 doi:10.20944/preprints202312.1571.v1

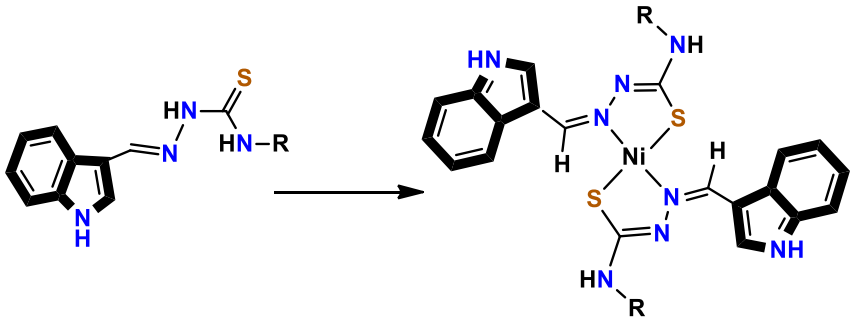

Figure 26. Synthesis of the complexes **114-117** from ligands **L34-L37**.

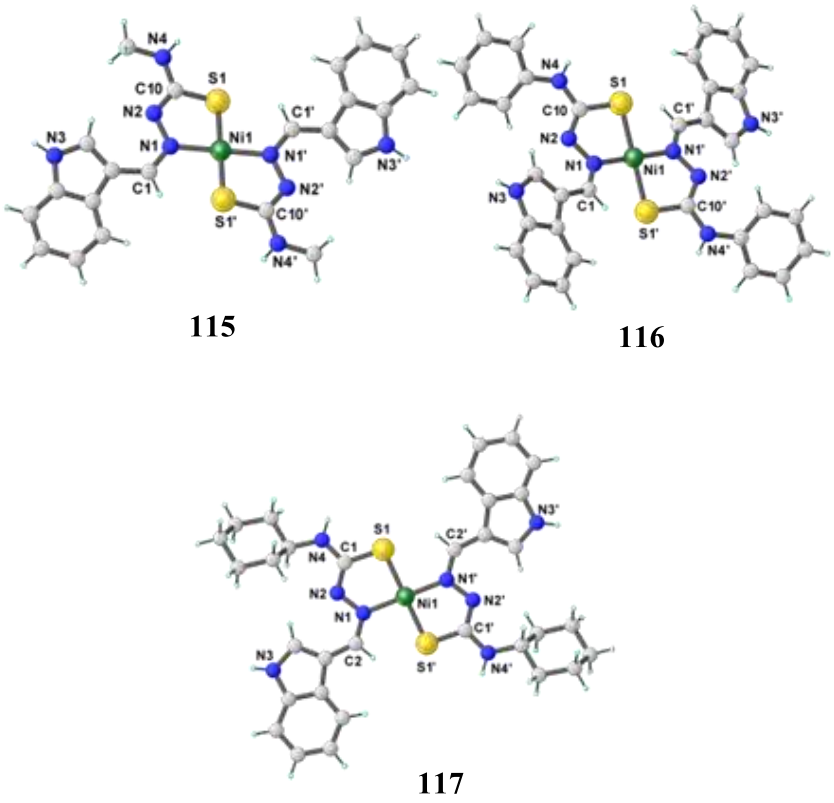

Figure 27. Crystal structure of the complexes **115**, **116** and **117**.

Pd^{II} complexes of indole-3-carbaldehyde thiosemicarbazones ([PdCl(L)(PPh_3)] (**118-122**) and [$Pd(L)_2$] (**123** and **124**; Figure 28), were synthesized from ligands **L38-L42** (Figure 28) by the same authors [69]. The structure of the ligand (**L40**) and complexes (**119-122** and **123**) were determined by X-ray analysis which revealed distorted square planar geometries for the complexes in which the thiosemicarbazone moiety acts as a monobasic bidentate (NS−) ligand and is coordinated to the Pd^{II} ion in such a way that a five membered ring was formed and the remaining sites were occupied by one chlorine and one triphenylphosphine (Figure 29). On the contrary, complex **123** adopted a square-planar geometry, forming two five-membered rings in which two indole-bound thiosemicarbazone ligands are coordinated to the Pd^{II} ion in a trans fashion. The complexes bound efficiently to CT-DNA via intercalative binding mode and cleaved significantly the DNA (pUC19 and pBR322) with no presence of co-oxidant at pH 7.2 and temperature 37 °C. Their DNA-binding affinity followed the order **121** > **122** > **120** > **118** > **119**. The higher binding propensity of the complexes **121** and **122** which might be due to the presence of bulky cyclohexyl and phenyl groups in the N-terminal position,

Preprints (www.preprints.org) | NOT PEER-REVIEWED | Posted: 20 December 2023 doi:10.20944/preprints202312.1571.v1

respectively. Additionally, the antiproliferative activity of the complexes against HepG-2, A549 and MCF7 cancer cells and one normal cell line (L929) was evaluated. All complexes exhibited acceptable cytotoxicity only against HepG-2 cells. In particular, complexes **121** and **122** containing the triphenylphosphine group showed the highest activity with IC_{50} value of 22.8 and 67.1 μM, respectively. Furthermore, complex **121** exhibited an activity almost equivalent to that of cisplatin. Noteworthy, the toxicity of all the complexes towards the normal cell line was lower than that found towards the tumor cell lines [69].

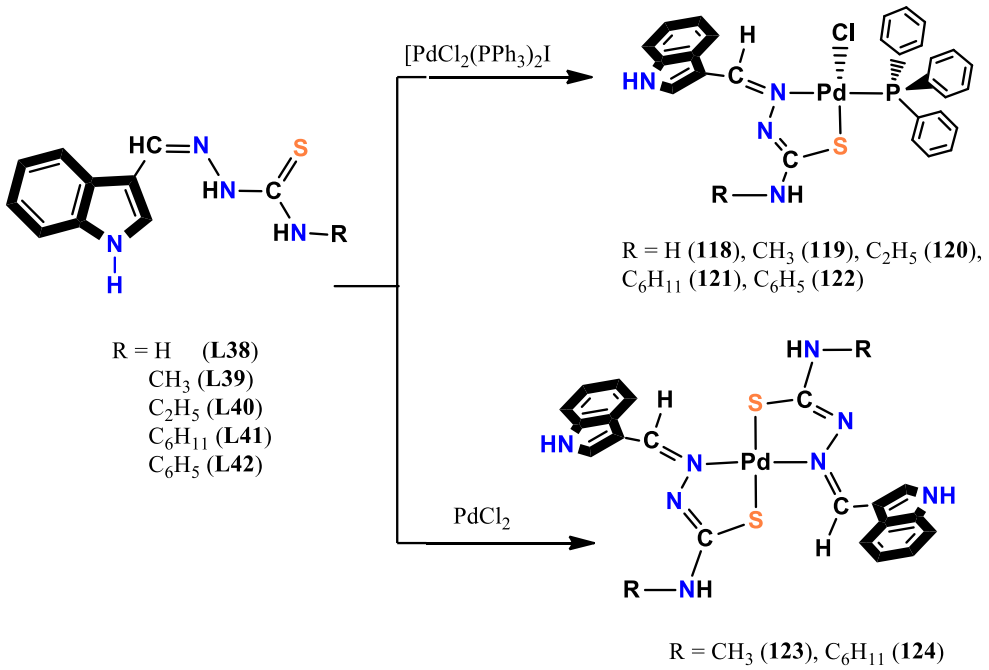

Figure 28. Synthesis of the complexes **118-124** from ligands **L38-L42**.

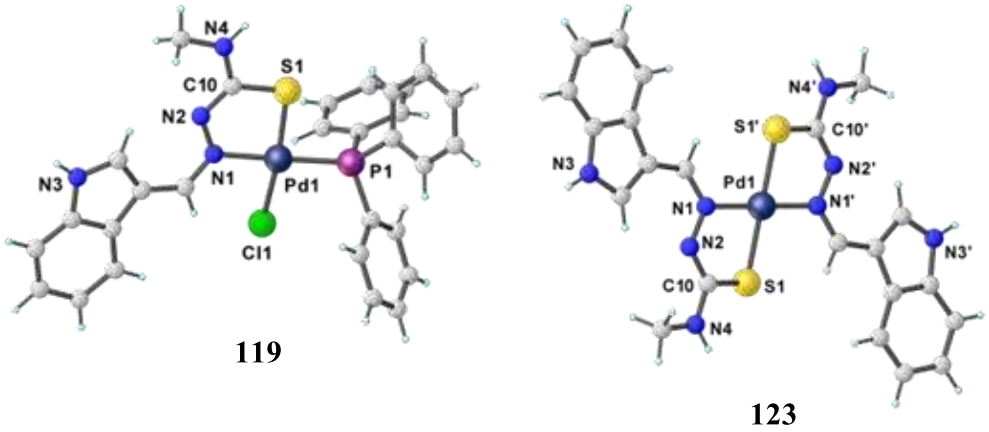

Figure 29. Crystal structure of the complexes **119** and **123**.

More recently, the research group of Jebiti Haribabu carried out a study on a water-soluble binuclear organometallic Ru(II)-p-cymene complex ($[Ru(\eta^6\text{-p-cymene})(\eta^2\text{-L})]_2$, (**125**; Figure 30) prepared from the reaction of (E)-2-((1H-indol-3-yl)methylene)-N-phenylhydrazine-1-carbothioamide (**L43**) with $[RuCl_2(p\text{-cymene})]_2$ and its structure was analyzed by UV–Vis, FT-IR, NMR and mass spectroscopic analyses [69]. In addition, the structure of the binuclear complex was determined by X-ray crystallography (Figure 31). Based on the data obtained, a pseudo-octahedral geometry has been hypothesized for the Ru(II) complex with the auxiliary ligand p-cymene and a (N,S) TSC chelating ligand located around each Ru(II) ion which, in turn, is connected by two-

Preprints (www.preprints.org) | NOT PEER-REVIEWED | Posted: 20 December 2023 doi:10.20944/preprints202312.1571.v1

bridged sulfur atoms of the TSC ligands. The antiproliferative assay (MTT method) performed for both the ligand its related complex **125** against A549-lung, MCF-7-breast, HeLa-cervical, HepG-2-liver, T24-urinary bladder and EA.hy926-endothelial cancer cells, and Vero-kidney epithelial normal cells highlighted significant activity for the complex against A549, HeLa and T24 cancer cells, with IC_{50} values lower than that of cisplatin (e.g. complex → IC_{50} = 7.70 μM vs. cisplatin → IC_{50} = 18.0 μM in A549), (complex → IC_{50} = 11.2 μM vs. cisplatin → IC_{50} = 22.4 μM in HeLa cells) and (complex → IC_{50} = 5.05 μM vs. cisplatin → IC_{50} = >50 μM in T24 cells). Moreover, the authors carried out in silico molecular docking studies which suggested that the two compounds might be investigated as antiviral agents since they showed potential binding to the spike protein and main protease of SARS-CoV-2. [68].

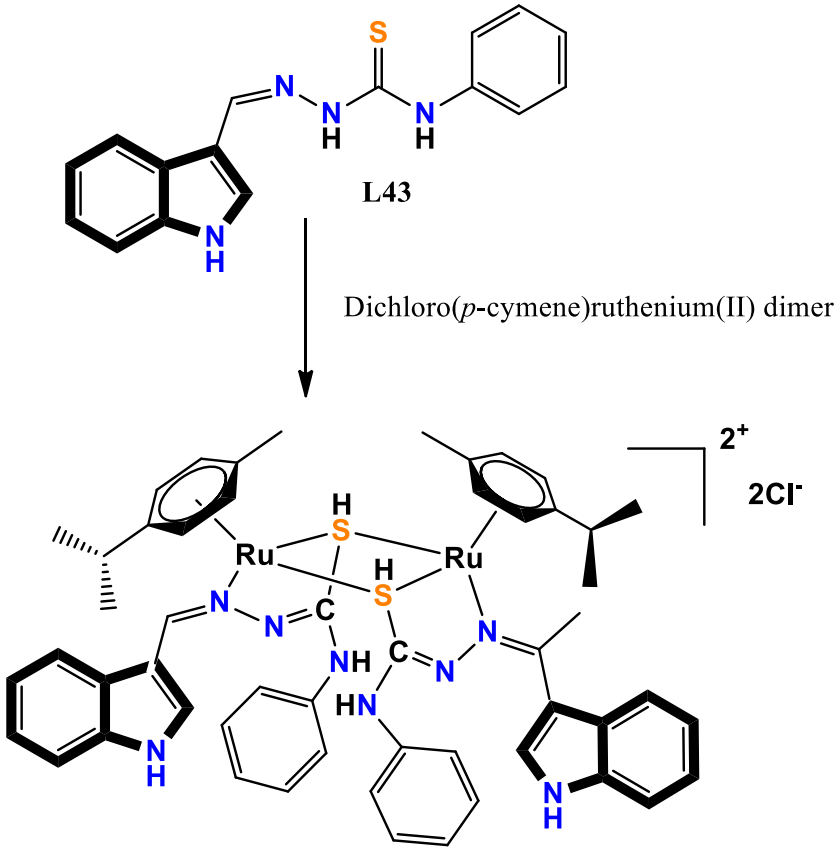

125

Figure 30. Synthesis of the complex **125** from ligand **L43**.

Preprints (www.preprints.org) | NOT PEER-REVIEWED | Posted: 20 December 2023 doi:10.20944/preprints202312.1571.v1

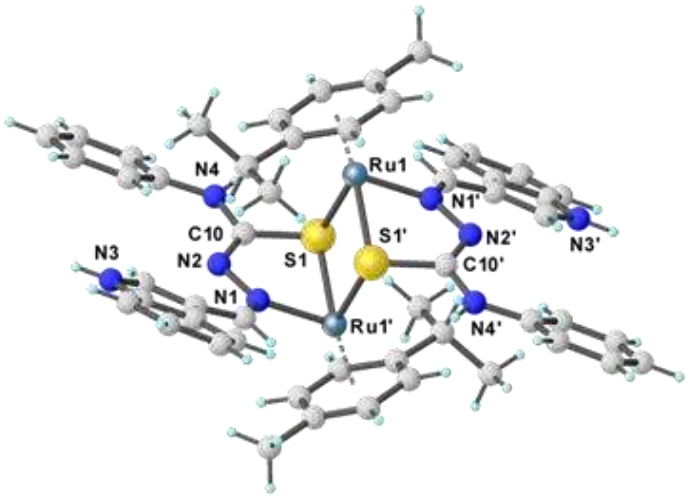

125

Figure 31. Crystal structure of the complex **125**.

Ru(II) complexes **126-129** were synthesized from O-R-1H-indole-2-carbothioate ligands **L48–L51** (which were obtained in turn from ligands **L44-L47**; Figure 32) and characterized using ^{1}H and ^{13}C NMR spectroscopy, and high-resolution ESI-MS. Moreover, ligand **L47,** complexes **127**, **128** and **129** were analyzed by single-crystal X-ray diffraction (Figure 33) which revealed that the complexes adopt pseudo-octahedral structures in which there are a η6-p-cymene ring, a N,S-chelated indole and chloride ion to make 18-electron complexes with "piano-stool" geometry. All complexes were tested as antibiotic agents against Mycobacterium abscessus NCTC 13031, Escherichia coli ATCC 11775, I469 ESBL, J53 2138E, J53 2140E, Staphylococcus aureus ATCC 29213, Acinetobacter baumannii NCTC 12156, Salmonella enterica serovar typhi and Mycobacterium tuberculosis H37Rv. The antimicrobial assays showed that complex **128** was the most effective derivative as it inhibited nine out of the twelve organisms tested; to follow, the most active derivative was found to be complex **127**. This outcome might be ascribed the steric hindrance of the R alkyl group on the indole ring which in turn may have an effect on aquation rate and degree of diffusion across biological barriers. Additionally, complexes **126, 127** and **128** exhibited moderate cytotoxicity against A2780 and A2780cisR cancer cell lines (assessed by MTT assay) and even lower activity (~ 2-3 folds) towards normal prostate epithelial cells PNT2 [70].

Preprints (www.preprints.org) | NOT PEER-REVIEWED | Posted: 20 December 2023 doi:10.20944/preprints202312.1571.v1

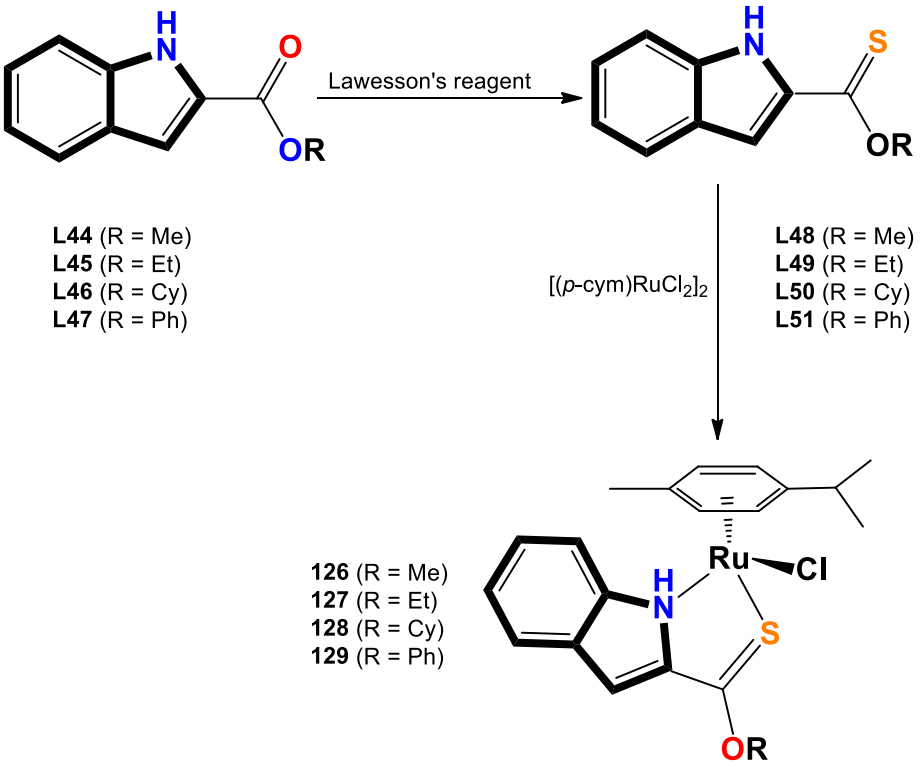

Figure 32. Synthesis of the complexes **126-129** from ligands **L44-L51**.

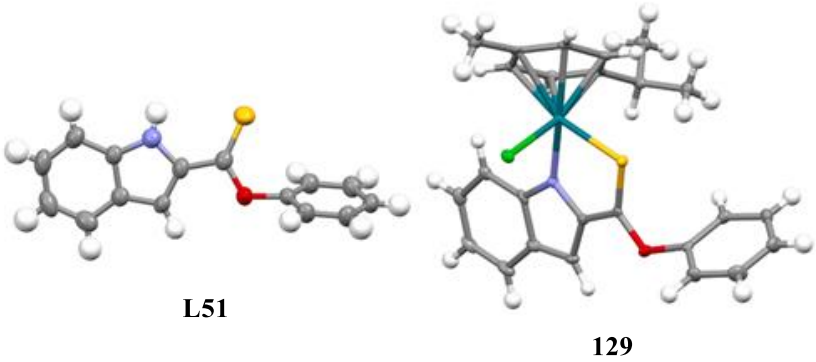

Figure 33. Crystal structure of the ligand **L51** and complex **129**.

Four Zn(II) complexes (i.e. **130**-**133**; Figure 34) composing of the zinc ion coordinated by two indole-based thiosemicarbazone ligands (i.e. **L52**-**L55**; Figure 34) were designed and synthesized by N. Balakrishnan et al. [71]. They were characterized by spectroscopic techniques such as UV–Vis, FT-IR, ^{1}H NMR, ^{13}C NMR and MS. The structures of **13**0 and **132** were determined by X-ray diffraction methods and showed that in both of them Zn^{2+}, in a distorted tetrahedral environment, was coordinated to the azomethine N and thiocarbonyl S atoms. The indole-thiosemicarbazone ligand acted as a bidentate ligand, with two of them coordinate with the Zn(II) ion (Figure 35). Moreover, the investigation of the binding affinity of the complexes with DNA was carried out by UV–Vis spectroscopy and viscosity measurements which indicated that complex **133** had the strongest DNA binding ability although they all preferred a DNA intercalation mechanism. These complexes showed also efficient BSA-binding through static quenching mechanism; complex **133**, however, bound more strongly than the other complexes. The cytotoxicity studies, evaluated by MTT method using two human cancer cell lines (A549 and MCF7), two human non-tumorigenic (MCF-10A and HEK-293) and one non-cancerous mouse fibroblasts (L929) cell line, revealed that complex **133** was the most effective derivative against A549 and MCF7 cells with IC_{50} = 37.9 and 60.3 μM, respectively. Its

Preprints (www.preprints.org) | NOT PEER-REVIEWED | Posted: 20 December 2023 doi:10.20944/preprints202312.1571.v1

cytotoxicity was comparable to that of cisplatin and, more importantly, complex **132** and **133** showed remarkable tumor selectivity [70].

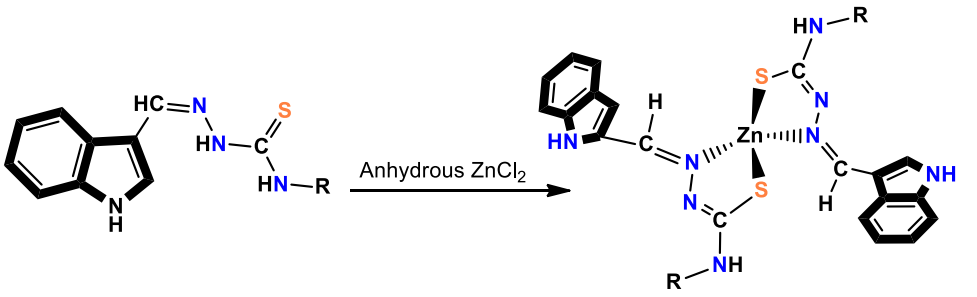

R = H (**L52**), CH_3 (**L53**), C_2H_5 (**L54**), C_6H_{11} (**L55**) R = H (**130**), CH_3 (**131**), C_2H_5 (**132**), C_6H_{11} (**133**)

Figure 34. Synthesis of the complexes **130-133** from ligands **L52-L55**.

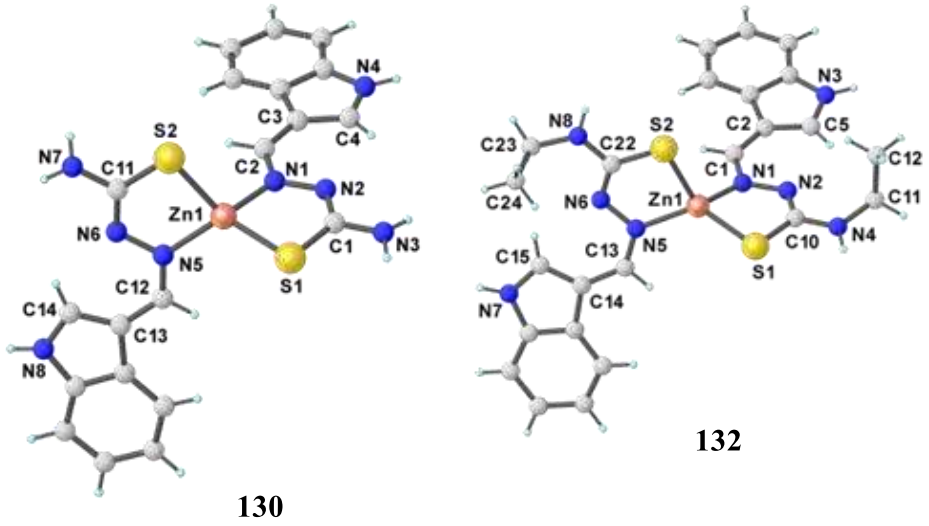

Figure 35. Crystal structure of the Zn(II) complexes **130** and **132**.

4. Conclusions

Indole-based metal complexes have showed to be able to successfully enhance selectivity and therapeutic efficiency. Their potential use in medicine has been demonstrated to be considerable, including anti-cancer, anti-tubercular, antiviral, and antibacterial applications. Coordination with various transition metals, such us Pd(II), Zn(II), Mn(II), Sn(IV), Co(II), Fe(II), Ni(II), Cu(I), Cu(II), Ir(II), Rh(II), Ag(I) and Ru(I) resulted in a considerable increase in the efficacy, as highlighted by several in vitro studies on different types of biological experiments (cell-based and enzymatic). In many cases the IC_{50} values were found to be lower than those of standard reference drugs. Both the presence of the indole scaffold and transition metal correlate with increased activity of the resulting complexes as evidenced also by computational studies. Characterization studies highlighted the impact of the presence of these two chemical features on the overall geometry of the complexes which in turn play a key role in the binding with biological targets. Furthermore, coordination with transition metals often determines a significant increase in the solubility of the complexes, thus leading to a better ADME profile and a consequent superior therapeutic potential.

The development of indole-based metal complexes and their enhanced activity may constitute a concrete opportunity to support the standard of care on various therapeutic approaches.

Funding: This research received no external funding. The APC was not applied as the article was written by Editor's invitation.

Institutional Review Board Statement: Not applicable.

Informed Consent Statement: Not applicable.

Data Availability Statement: Data sharing is not applicable to this article.

Conflicts of Interest: The authors declare no conflict of interest.

References

1. Lakhdar, S.; Westermaier, M.; Terrier, F.; Goumont, R.; Boubaker, T.; Ofial, A. R.; Mayr, H., Nucleophilic reactivities of indoles. *The Journal of organic chemistry* **2006,** 71, (24), 9088-9095.
2. Ma, Q.; Zhang, X.; Qu, Y., Biodegradation and biotransformation of indole: advances and perspectives. *Frontiers in microbiology* **2018,** 9, 2625.
3. Mondal, D.; Kalar, P. L.; Kori, S.; Gayen, S.; Das, K., Recent developments on synthesis of indole derivatives through green approaches and their pharmaceutical applications. *Current Organic Chemistry* **2020,** 24, (22), 2665-2693.
4. Heravi, M. M.; Amiri, Z.; Kafshdarzadeh, K.; Zadsirjan, V., Synthesis of indole derivatives as prevalent moieties present in selected alkaloids. *RSC advances* **2021,** 11, (53), 33540-33612.
5. Sarkar, D.; Amin, A.; Qadir, T.; Sharma, P. K., Synthesis of medicinally important indole derivatives: A Review. *The Open Medicinal Chemistry Journal* **2021,** 15, (1).
6. Chen, L.; Zou, Y.-X., Recent progress in the synthesis of phosphorus-containing indole derivatives. *Organic & Biomolecular Chemistry* **2018,** 16, (41), 7544-7556.
7. Bischler, A., Ueber die entstehung einiger substituirter indole. *Berichte der deutschen chemischen Gesellschaft* **1892,** 25, (2), 2860-2879.
8. Fischer, E.; Jourdan, F., Ueber die hydrazine der brenztraubensäure. *Berichte der deutschen chemischen Gesellschaft* **1883,** 16, (2), 2241-2245.
9. Hemetsberger, H.; Knittel, D., Synthesis and thermolysis of α-azidoacrylates (ene-azides, IV) Enazide, 4. Mitt. *Monatshefte für Chemie/Chemical Monthly* **1972,** 103, 194-204.
10. Baudin, J.-B.; Julia, S. A., Synthesis of indoles from N-aryl-1-alkenylsulphinamides. *Tetrahedron letters* **1986,** 27, (7), 837-840.
11. Dorababu, A., Indole–a promising pharmacophore in recent antiviral drug discovery. *RSC Medicinal Chemistry* **2020,** 11, (12), 1335-1353.
12. Al Awadh, A. A., Biomedical applications of selective metal complexes of Indole, Benzimidazole, Benzothiazole and Benzoxazole: A review (From 2015 to 2022). *Saudi Pharmaceutical Journal* **2023**, 101698.
13. Zhang, M.-Z.; Chen, Q.; Yang, G.-F., A review on recent developments of indole-containing antiviral agents. *European journal of medicinal chemistry* **2015,** 89, 421-441.
14. Chadha, N.; Silakari, O., Indoles as therapeutics of interest in medicinal chemistry: Bird's eye view. *European Journal of Medicinal Chemistry* **2017,** 134, 159-184.
15. de Sa Alves, F. R.; Barreiro, E. J.; Manssour Fraga, C. A., From nature to drug discovery: the indole scaffold as a 'privileged structure'. *Mini reviews in medicinal chemistry* **2009,** 9, (7), 782-793.
16. Kumar, D.; Kumar, N. M.; Tantak, M. P.; Ogura, M.; Kusaka, E.; Ito, T., Synthesis and identification of α-cyano bis (indolyl) chalcones as novel anticancer agents. *Bioorganic & medicinal chemistry letters* **2014,** 24, (22), 5170-5174.
17. Shimazaki, Y.; Yajima, T.; Takani, M.; Yamauchi, O., Metal complexes involving indole rings: Structures and effects of metal–indole interactions. *Coordination Chemistry Reviews* **2009,** 253, (3-4), 479-492.
18. Zhang, M.-Z.; Mulholland, N.; Beattie, D.; Irwin, D.; Gu, Y.-C.; Chen, Q.; Yang, G.-F.; Clough, J., Synthesis and antifungal activity of 3-(1, 3, 4-oxadiazol-5-yl)-indoles and 3-(1, 3, 4-oxadiazol-5-yl) methyl-indoles. *European Journal of Medicinal Chemistry* **2013,** 63, 22-32.
19. Lal, S.; J Snape, T., 2-Arylindoles: a privileged molecular scaffold with potent, broad-ranging pharmacological activity. *Current medicinal chemistry* **2012,** 19, (28), 4828-4837.
20. Wang, M.; Rakesh, K.; Leng, J.; Fang, W.-Y.; Ravindar, L.; Gowda, D. C.; Qin, H.-L., Amino acids/peptides conjugated heterocycles: A tool for the recent development of novel therapeutic agents. *Bioorganic chemistry* **2018,** 76, 113-129.
21. Bajad, N. G.; Singh, S. K.; Singh, S. K.; Singh, T. D.; Singh, M., Indole: A promising scaffold for the discovery and development of potential anti-tubercular agents. *Current Research in Pharmacology and Drug Discovery* **2022**, 100119.
22. Fang, W.-Y.; Ravindar, L.; Rakesh, K.; Manukumar, H.; Shantharam, C.; Alharbi, N. S.; Qin, H.-L., Synthetic approaches and pharmaceutical applications of chloro-containing molecules for drug discovery: A critical review. *European journal of medicinal chemistry* **2019,** 173, 117-153.
23. Pacheco, P. A.; Santos, M. M., Recent progress in the development of indole-based compounds active against malaria, trypanosomiasis and leishmaniasis. *Molecules* **2022,** 27, (1), 319.

24. Moku, B.; Ravindar, L.; Rakesh, K.; Qin, H.-L., The significance of N-methylpicolinamides in the development of anticancer therapeutics: Synthesis and structure-activity relationship (SAR) studies. *Bioorganic Chemistry* **2019,** 86, 513-537.
25. Bianucci, A. M.; Da Settimo, A.; Da Settimo, F.; Primofiore, G.; Martini, C.; Giannaccini, G.; Lucacchini, A., Benzodiazepine receptor affinity and interaction of some N-(indol-3-ylglyoxylyl) amine derivatives. *Journal of medicinal chemistry* **1992,** 35, (12), 2214-2220.
26. Singh, D.; Grover, V.; Kumar, K.; Jain, K., Metal ion prompted macrocyclic complexes derived from indole-2, 3-dione (isatin) and O-phenylenediamine with their spectroscopic and antibacterial studies. *Acta Chimica Slovenica* **2010,** 57, (4), 775-780.
27. Vendeville, S.; Lin, T.-I.; Hu, L.; Tahri, A.; McGowan, D.; Cummings, M. D.; Amssoms, K.; Canard, M.; Last, S.; Van den Steen, I., Finger loop inhibitors of the HCV NS5b polymerase. Part II. Optimization of tetracyclic indole-based macrocycle leading to the discovery of TMC647055. *Bioorganic & medicinal chemistry letters* **2012,** 22, (13), 4437-4443.
28. Au, V. S.; Bremner, J. B.; Coates, J.; Keller, P. A.; Pyne, S. G., Synthesis of some cyclic indolic peptoids as potential antibacterials. *Tetrahedron* **2006,** 62, (40), 9373-9382.
29. Álvarez, R.; López, V.; Mateo, C.; Medarde, M.; Peláez, R., New para–para stilbenophanes: Synthesis by McMurry coupling, conformational analysis and inhibition of tubulin polymerisation. *Chemistry–A European Journal* **2011,** 17, (12), 3406-3419.
30. Neochoritis, C. G.; Miraki, M. K.; Abdelraheem, E. M.; Surmiak, E.; Zarganes-Tzitzikas, T.; Łabuzek, B.; Holak, T. A.; Dömling, A., Design of indole-and MCR-based macrocycles as p53-MDM2 antagonists. *Beilstein Journal of Organic Chemistry* **2019,** 15, (1), 513-520.
31. Chen, R. Synthesis of novel Indole-based Macrocycles. UNSW Sydney, 2012.
32. Cheekatla, S. R.; Barik, D.; Anand, G.; Mol KM, R.; Porel, M., Indole-Based Macrocyclization by Metal-Catalyzed Approaches. *Organics* **2023,** 4, (3), 333-363.
33. Zhang, Y.-C.; Jiang, F.; Shi, F., Organocatalytic asymmetric synthesis of indole-based chiral heterocycles: strategies, reactions, and outreach. *Accounts of chemical research* **2019,** 53, (2), 425-446.
34. Lin, C.-H.; Wu, Y.-R.; Kung, P.-J.; Chen, W.-L.; Lee, L.-C.; Lin, T.-H.; Chao, C.-Y.; Chen, C.-M.; Chang, K.-H.; Janreddy, D., The potential of indole and a synthetic derivative for polyQ aggregation reduction by enhancement of the chaperone and autophagy systems. *ACS Chemical Neuroscience* **2014,** 5, (10), 1063-1074.
35. Kung, P.-J.; Tao, Y.-C.; Hsu, H.-C.; Chen, W.-L.; Lin, T.-H.; Janreddy, D.; Yao, C.-F.; Chang, K.-H.; Lin, J.-Y.; Su, M.-T., Indole and synthetic derivative activate chaperone expression to reduce polyQ aggregation in SCA17 neuronal cell and slice culture models. *Drug design, development and therapy* **2014**, 1929-1939.
36. Chen, C.-M.; Chen, W.-L.; Hung, C.-T.; Lin, T.-H.; Chao, C.-Y.; Lin, C.-H.; Wu, Y.-R.; Chang, K.-H.; Yao, C.-F.; Lee-Chen, G.-J., The indole compound NC009-1 inhibits aggregation and promotes neurite outgrowth through enhancement of HSPB1 in SCA17 cells and ameliorates the behavioral deficits in SCA17 mice. *Neurotoxicology* **2018,** 67, 259-269.
37. Wei, P.-C.; Lee-Chen, G.-J.; Chen, C.-M.; Wu, Y.-R.; Chen, Y.-J.; Lin, J.-L.; Lo, Y.-S.; Yao, C.-F.; Chang, K.-H., Neuroprotection of indole-derivative compound NC001-8 by the regulation of the NRF2 pathway in Parkinson's disease cell models. *Oxidative medicine and cellular longevity* **2019,** 2019.
38. Afanas'eva, I. B.; Ostrakhovitch, E. A.; Mikhal'chik, E. V.; Ibragimova, G. A.; Korkina, L. G., Enhancement of antioxidant and anti-inflammatory activities of bioflavonoid rutin by complexation with transition metals. *Biochemical pharmacology* **2001,** 61, (6), 677-684.
39. Ejidike, I. P.; Ajibade, P. A., Synthesis, characterization and biological studies of metal (II) complexes of (3 E)-3-[(2-{(E)-[1-(2, 4-dihydroxyphenyl) ethylidene] amino} ethyl) imino]-1-phenylbutan-1-one Schiff base. *Molecules* **2015,** 20, (6), 9788-9802.
40. Zhu, X.; Li, Y.; Wei, Y.; Wang, S.; Zhou, S.; Zhang, L., Reactivity of 3-imino-functionalized indoles with rare-earth-metal amides: Unexpected substituent effects on C–H activation pathways and assembly of rare-earth-metal complexes. *Organometallics* **2016,** 35, (11), 1838-1846.
41. Abdulghani, A. J.; Hussain, R. K., Synthesis and Characterization of Schiff Base Metal Complexes Derived from Cefotaxime with 1H-indole-2, 3-dione (Isatin) and 4-N, N-dimethyl-aminobenzaldehyde. *Open Journal of Inorganic Chemistry* **2015,** 5, (04), 83.
42. EL-Gammal, O. A.; Alshater, H.; El-Boraey, H. A., Schiff base metal complexes of 4-methyl-1H-indol-3-carbaldehyde derivative as a series of potential antioxidants and antimicrobial: Synthesis, spectroscopic characterization and 3D molecular modeling. *Journal of Molecular Structure* **2019,** 1195, 220-230.
43. Deng, X.-j.; Yu, Q.; Bian, H.-D.; Ju, H.-D.; Wang, B.-L., Syntheses, structures and properties of complexes of indole-3-propionic acid. *Transition Metal Chemistry* **2016,** 41, 591-598.
44. Yamamoto, K.; Kimura, S.; Murahashi, T., σ–π Continuum in indole–Palladium (II) complexes. *Angewandte Chemie International Edition* **2016,** 55, (17), 5322-5326.
45. Shimazaki, Y.; Yajima, T.; Yamauchi, O., Properties of the indole ring in metal complexes. A comparison with the phenol ring. *Journal of Inorganic Biochemistry* **2015,** 148, 105-115.

46. Yamauchi, O.; Takani, M.; Toyoda, K.; Masuda, H., Indole nitrogen-palladium (II) bonding. Chemical and structural characterization of palladium (II) complexes of alkylindoles and intermediacy of the 3H-indole ring. *Inorganic Chemistry* **1990,** 29, (10), 1856-1860.
47. Oberhuber, N.; Ghosh, H.; Nitzsche, B.; Dandawate, P.; Höpfner, M.; Schobert, R.; Biersack, B., Synthesis and Anticancer Evaluation of New Indole-Based Tyrphostin Derivatives and Their (p-Cymene) dichloridoruthenium (II) Complexes. *International Journal of Molecular Sciences* **2023,** 24, (1), 854.
48. Khan, A.; Jasinski, J. P.; Smolenski, V. A.; Hotchkiss, E. P.; Kelley, P. T.; Shalit, Z. A.; Kaur, M.; Paul, K.; Sharma, R., Enhancement in anti-tubercular activity of indole based thiosemicarbazones on complexation with copper (I) and silver (I) halides: structure elucidation, evaluation and molecular modelling. *Bioorganic Chemistry* **2018,** 80, 303-318.
49. Chilwal, A.; Malhotra, P.; Narula, A., Synthesis, characterization, thermal, and antibacterial studies of organotin (IV) complexes of indole-3-butyric acid and indole-3-propionic acid. *Phosphorus, Sulfur, and Silicon and the Related Elements* **2014,** 189, (3), 410-421.
50. Li, J.; Gao, T.; Zhang, W.; Sun, W.-H., Synthesis and characterization of 2-imino-indole nickel complexes and their ethylene oligomerization study. *Inorganic Chemistry Communications* **2003,** 6, (11), 1372-1374.
51. Soldevila-Barreda, J. J.; Fawibe, K. B.; Azmanova, M.; Rafols, L.; Pitto-Barry, A.; Eke, U. B.; Barry, N. P., Synthesis, characterisation and in vitro anticancer activity of catalytically active indole-based half-sandwich complexes. *Molecules* **2020,** 25, (19), 4540.
52. Babijczuk, K.; Warżajtis, B.; Starzyk, J.; Mrówczyńska, L.; Jasiewicz, B.; Rychlewska, U., Synthesis, Structure and Biological Activity of Indole–Imidazole Complexes with ZnCl2: Can Coordination Enhance the Functionality of Bioactive Ligands? *Molecules* **2023,** 28, (10), 4132.
53. Lo, K. K.-W.; Tsang, K. H.-K.; Hui, W.-K.; Zhu, N., Synthesis, characterization, crystal structure, and electrochemical, photophysical, and protein-binding properties of luminescent rhenium (I) diimine indole complexes. *Inorganic chemistry* **2005,** 44, (17), 6100-6110.
54. Wittmann, C.; Sivchenko, A. S.; Bacher, F.; Tong, K. K.; Guru, N.; Wilson, T.; Gonzales, J.; Rauch, H.; Kossatz, S.; Reiner, T., Inhibition of microtubule dynamics in cancer cells by indole-modified latonduine derivatives and their metal complexes. *Inorganic Chemistry* **2022,** 61, (3), 1456-1470.
55. Sahar, Y. J.; Mohammed, H.; Al-Abady, Z. N., Synthesis and characterization of new metal complexes containing azo-indole moiety and anti-leukemia human (HL-60) study of its palladium (II) complex. *Results in Chemistry* **2023,** 5, 100847.
56. K. Bhanumathy, K.; Balagopal, A.; Vizeacoumar, F. S.; Vizeacoumar, F. J.; Freywald, A.; Giambra, V., Protein tyrosine kinases: their roles and their targeting in leukemia. *Cancers* **2021,** 13, (2), 184.
57. Babahan, I.; Özmen, A.; Aksel, M.; Bilgin, M. D.; Gumusada, R.; Gunay, M. E.; Eyduran, F., A novel bidentate ligand containing oxime, hydrazone and indole moieties and its BF2+ bridged transition metal complexes and their efficiency against prostate and breast cancer cells. *Applied Organometallic Chemistry* **2020,** 34, (7), e5632.
58. Alanazi, R. L.; Zaki, M.; Bawazir, W. A., Synthesis and characterization of new metal complexes containing Triazino [5, 6–b] indole moiety: In vitro DNA and HSA binding studies. *Journal of Molecular Structure* **2021,** 1246, 131203.
59. Shakir, Y. G.; Shamran, M. H., Synthesis and characterization of indole azo metal complexes and study of their biological activity. *Res. J. Chem. Environ.* **2022,** 2022, 12.
60. Tümer, M., Synthesis and spectral characterization of metal complexes containing tetra-and pentadentate Schiff base ligands. *Sythesis and Reactivity in Inorganic and Matel-Organic Chemistry* **2000,** 30, (6), 1139-1158.
61. Arunadevi, A.; Raman, N., Indole-derived water-soluble N, O bi-dentate ligand-based mononuclear transition metal complexes: in silico and in vitro biological screening, molecular docking and macromolecule interaction studies. *Journal of Biomolecular Structure and Dynamics* **2019**.
62. Daina, A.; Michielin, O.; Zoete, V., SwissADME: a free web tool to evaluate pharmacokinetics, drug-likeness and medicinal chemistry friendliness of small molecules. *Scientific reports* **2017,** 7, (1), 42717.
63. Varma, R. R.; Pandya, J. G.; Vaidya, F. U.; Pathak, C.; Bhatt, B. S.; Patel, M. N., Biological activities of pyrazoline-indole based Re (I) carbonyls: DNA interaction, antibacterial, anticancer, ROS production, lipid peroxidation, in vivo and in vitro cytotoxicity studies. *Chemico-Biological Interactions* **2020,** 330, 109231.
64. Sharma, S.; Meena, R.; Satyawana, Y.; Fahmi, N., Manganese (II) complexes of biological relevance: Synthesis and spectroscopic characterization of novel manganese (II) complexes with monobasic bidentate ligands derived from halo-substituted 1 H-indole-2, 3-diones. *Russian Journal of General Chemistry* **2016,** 86, 2807-2816.
65. Seifullina, I.; Skorokhod, L.; Pulya, A.; Vlasenko, V.; Trigub, A.; Rakipow, I., Synthesis, Structure, and Properties of Co 2+ and Ni 2+ Complexes with the Product of Condensation of 2-(7-Bromo-2-oxo-5-phenyl-3 H-1, 4-benzodiazepin-1-yl) acetohydrazide and 1 H-Indole-2, 3-dione. *Russian Journal of General Chemistry* **2020,** 90, 1298-1303.

 doi:10.20944/preprints202312.1571.v1

66. Devi, J.; Yadav, J.; Kumar, D.; Jindal, D. K.; Basu, B., Synthesis, spectral analysis and in vitro cytotoxicity of diorganotin (IV) complexes derived from indole-3-butyric hydrazide. *Applied Organometallic Chemistry* **2020,** 34, (10), e5815.
67. Lau, J. S.-Y.; Lee, P.-K.; Tsang, K. H.-K.; Ng, C. H.-C.; Lam, Y.-W.; Cheng, S.-H.; Lo, K. K.-W., Luminescent cyclometalated iridium (III) polypyridine indole complexes◎ synthesis, photophysics, electrochemistry, protein-binding properties, cytotoxicity, and cellular uptake. *Inorganic Chemistry* **2009,** 48, (2), 708-718.
68. Haribabu, J.; Jeyalakshmi, K.; Arun, Y.; Bhuvanesh, N. S.; Perumal, P. T.; Karvembu, R., Synthesis of Ni (II) complexes bearing indole-based thiosemicarbazone ligands for interaction with biomolecules and some biological applications. *JBIC Journal of Biological Inorganic Chemistry* **2017,** 22, 461-480.
69. Haribabu, J.; Tamizh, M. M.; Balachandran, C.; Arun, Y.; Bhuvanesh, N. S.; Endo, A.; Karvembu, R., Synthesis, structures and mechanistic pathways of anticancer activity of palladium (II) complexes with indole-3-carbaldehyde thiosemicarbazones. *New Journal of Chemistry* **2018,** 42, (13), 10818-10832.
70. Nolan, V. C.; Rafols, L.; Harrison, J.; Soldevila-Barreda, J. J.; Crosatti, M.; Garton, N. J.; Wegrzyn, M.; Timms, D. L.; Seaton, C. C.; Sendron, H., Indole-containing arene-ruthenium complexes with broad spectrum activity against antibiotic-resistant bacteria. *Current research in microbial sciences* **2022,** 3, 100099.
71. Balakrishnan, N.; Haribabu, J.; Krishnan, D. A.; Swaminathan, S.; Mahendiran, D.; Bhuvanesh, N. S.; Karvembu, R., Zinc (II) complexes of indole thiosemicarbazones: DNA/protein binding, molecular docking and in vitro cytotoxicity studies. *Polyhedron* **2019,** 170, 188-201.